

2mip

Final Technical Report

NASA Grant NGR-05-009-180

Professor P.M. Banks

Dr. J.R. Doupnik

Principal Investigators

NASA-CR-137371) [STUDIES OF THE
STRUCTURE OF THE PLASMASPHERE AS SEEN BY
RADIOSOUNDER MEASUREMENTS ABOARD THE
ALOVETTI-SATELLITE] Final (California
Univ.) 74 p HC \$6.75 CSCL 03B

N74-20467

Unclas

G3/30 16078

November 13, 1973

Under the terms of this grant, studies were made of the structure of the plasmasphere as seen by radiosounder measurements aboard the Alovetti-II satellite. During the early phases of the work, magnetic tape data files were obtained from the NASA Ames Research Center to give a reasonably complete set of high latitude electron density profiles. Owing to internal data processing difficulties, Ames was able to provide these data only after considerable delay (8 months).

During the period between the initial data request and data availability, considerable effort was expended to develop models of ion flow in the topside ionosphere. These models took both H^+ and O^+ into account and permitted various parameter studies to be made of the various factors which affect H^+ escape in polar wind flows. The results of these studies were published as an initial paper in the 1972 "Critical Problems in Magnetospheric Physics" symposium held in Madrid, Spain. A copy of this paper is included here as Attachment I.

When the NASA data became available, extensive computer programs were written to display the measured electron density profiles in ways useful to geophysical analysis. It was found that the expected mid-latitude trough was easily discernable in the nighttime ionosphere at locations expected from similar observations of the plasmopause. In the dayside ionosphere, however, it proved extremely difficult to find any trough-like phenomena in the electron density. Using the previously developed computer models, it was possible to study the region where the plasmopause appeared to be absent. It was found that over much of the dayside, large H^+ fluxes were computed well inside the plasmopause extending down to L-shells as

as low as 2.5. This morning flow has been described in detail as a paper given as Attachment II which will soon appear in Planetary and Space Science.

Further studies were undertaken to develop ideas concerning the relation between the location of the plasmapause as it is found in the equatorial plane and the location of the ionospheric trough. Briefly, it was found that a good correspondence can be expected only in the nightside during periods of moderate to disturbed magnetic activity. In the dayside the trough is at lower latitudes than the plasmasphere owing to the way H^+ must replenish magnetic field tubes of considerable volume. A paper discussing this effect has been submitted to the Journal of Geophysical Research and is included here as Attachment III.

ATTACHMENT I

BEHAVIOR OF THERMAL PLASMA IN THE MAGNETOSPHERE AND TOPSIDE IONOSPHERE

Peter M. Banks

Department of Applied Physics and Information Science
University of California, San Diego
La Jolla, California 92037
U.S.A.

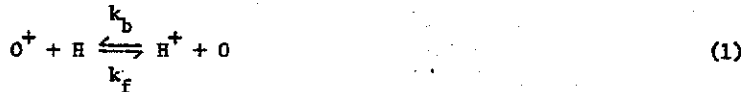
Introduction

Radio measurements of whistlers in the early 1950's [1] provided the first direct evidence for substantial amounts of thermal plasma ($n_e \sim 500/\text{cm}^3$) at altitudes of several earth radii. Using the charge exchange reaction of Dungey [2], Johnson [3] identified this plasma as H^+ of ionospheric origin. Further interest in the plasma of these very high regions was spurred by the spacecraft [4] and radio whistler [5] discoveries of the plasmopause, and the realization that the high density plasma envelope surrounding the earth was shaped in the form of a distorted torus [6].

Many of the early ideas about the plasmasphere tended to ignore obvious connection between the ionosphere and the thermal particles at large distances from the earth. Although it was often thought that the transition from the O^+ of the upper F_2 -region to the H^+ of the magnetosphere could be described in terms of quiescent equilibrium of a diffusive character, recent measurements [7] and theory [8] suggest the existence of far more dynamic flow states throughout much of the magnetosphere. It is this dynamic behavior which is the topic of the present review. Although the varieties of thermal plasma behavior are considerable, it now appears that many puzzling plasma features of the plasmasphere, the high latitude polar regions and the global topside ionosphere can be explained in a qualitative, and sometimes quantitative sense.

To set the stage for this review, Figure 1 shows a recent model of the magnetospheric environment. Of special interest for the thermal plasma behavior is the plasmopause, a sharp gradient in electron density aligned perpendicular to magnetic L-shells ranging from $L = 4$ in the morning sector to $L = 7$ in the afternoon. A schematic diagram of the equatorial projection of the plasmopause is given by Figure 2, taken from the work of Chappell, et al. [9].

There appears to be little doubt that the principal factors involved in the formation of a plasmopause are the general cross tail magnetospheric electric field, the co-rotation induced terrestrial electric field, and the existence of a finite rate at which the ionosphere can provide thermal plasma to the magnetosphere. A simple model of the plasmopause can be constructed in the following way: The principal thermal ion of the topside ionosphere and magnetosphere is H^+ which has its origin in the upper F_2 -region from the charge exchange reaction



with rates $k_f = 2.5 \times 10^{-11} T_n^{1/2} \text{ cm}^3/\text{sec}$ and $k_b = 2.2 \times 10^{-11} T_i^{1/2} \text{ cm}^3/\text{sec}$ determined from recent experiments [10].

In equilibrium, (1) gives the H^+/O^+ density ratio as

$$n(\text{H}^+)/n(\text{O}^+) = 9/8 n(\text{H})/n(\text{O}) (T_n/T_i)^{1/2}. \quad (2)$$

When an excess of H^+ is present owing to inward ion transport, Equation (1) acts as a sink, converting H^+ into O^+ . When there is a deficit of H^+ resulting from an outflow of ions, (1) acts as a source and tends to reduce the O^+ density. These actions are closely related to the diffusive character of the upper ionosphere and virtually all production or loss of H^+ occurs in the altitude range 550-900 km.

When unbalanced pressure gradients, gravity or other external forces are present, plasma flow is rapidly established along the magnetic field lines. In the absence of external electric fields transverse to \vec{B} , the plasma flow is constrained to be parallel to \vec{B} and the steady state density distribution along a field line reflects the buoyancy of H^+ in O^+ with the lighter gas essentially floating upon the heavier as a result of gravitationally induced electric fields parallel to \vec{B} .

As changes occur in the pressure and density of the O^+ of the F_2 -region, variations propagate through the H^+ plasma and inward or outward flows may occur as the plasma system seeks a new equilibrium. For the most part, however, deviations in plasma density in the outer sections of the field tube are not large and a typical equatorial ion concentration is of the order $5 \times 10^2 \text{ cm}^{-3}$ to $5 \times 10^3 \text{ cm}^{-3}$.

To progress further with the model, suppose that beyond a certain latitude (or L shell) a transverse electric field is present. If properly oriented, such a field will drive plasma away from the earth in a direction orthogonal to \vec{E} and \vec{B} . If this field is sufficiently strong, the plasma will reach the magnetopause in a reasonably short period of time (6 to 12 hours) and will be permanently lost to the solar wind. The effect of this outward flow upon the ion density of the region exposed to \vec{E} will depend upon the rate at which ionization can flow out of the ionosphere to replace the ions drifting across magnetic field lines. For H^+ this flow is greatly restricted by collisions with O^+ in the regions below 1000 km altitude and, as a consequence, the ion density of the regions exposed to the magnetospheric convection electric field is very low ($n_e \approx 10^{-2} \text{ cm}^{-3}$) [9]. Comparing the characteristic ion densities for the relatively stationary H^+ and that which is subject to $\vec{E} \times \vec{B}$ drift, it is seen that the plasmopause represents the approximate limit of penetration of the magnetospheric convection electric field. However, as discussed later, conditions other than $\vec{E} \times \vec{B}$ drift can give rise to low H^+ densities in the transition zone of the topside ionosphere. In such cases, there is no simple relationship between the plasmopause as seen far from the earth and the ionization discontinuities seen in the ionosphere.

Making use of the foregoing ideas, it is possible to explain more clearly the meaning of Figure 2. In the tail of the magnetosphere, the convection electric field lies in the dawn to dusk direction and the thermal plasma flow is towards the earth, as indicated by the dotted plasma trajectories. Owing to the frozen field concept, there are two ways of viewing this motion. The first is to regard the plasma as being driven across fixed magnetic field lines. Plasma at any height above the equatorial plane is forced to move orthogonal to \vec{E} and \vec{B} which, in this case, implies not only a motion towards the sun, but also a velocity component towards the equatorial plane. Owing to the convergence of the magnetic field, there is a compression of the plasma which is not uniform along a given field line and parallel redistribution flows are needed to maintain the plasma parallel force balance. Although it is not obvious in this formulation, the fact that the magnetic field lines are equipotentials insures that the $\vec{E} \times \vec{B}$ velocity of plasma across a given field line varies in such a way that the plasma moves uniformly from one field line to the next.

The second formulation of the $\vec{E} \times \vec{B}$ drift problem is based on this last condition. Plasma and magnetic flux tubes are considered to move together with the plasma contained in a given field tube undergoing compressional and redistributive effects as the field tube itself moves under the influence of the external electric field. Plasma contained in a given field tube can be lost or replenished only through the feet of the field tube; i.e., a dipolar field tube acts as a reservoir of plasma which is free to flow parallel to \vec{B} in response to pressure gradients or other parallel components of external forces.

Returning to the diagram shown in Figure 2, the inward flow of plasma from the tail represents both a compression of ambient plasma and a net equatorward motion of plasma in the ionosphere. As the magnetospheric flow passes the morningside of the earth, no further changes in plasma density occur until the trajectories of the motion move away from the earth towards the magnetopause, when a simultaneous rarefaction and poleward motion of the ionosphere occur. Although the nightside compression and dayside rarefactions are real and important effects, the overall ion density in this outer convection region is very low owing to the very low plasma density in the tail of the magnetosphere. This, of course, is related to the relatively slow rate of ionospheric plasma replenishment.

Inside the plasmapause the magnetospheric convection electric field is mostly, but not completely, absent. As a consequence, the thermal plasma of the plasmasphere tends to rotate with the earth, or at least with the atmospheric regions between 100 to 150 km where dynamo electric fields are generated. Owing to the influence of the convection electric field the idea of co-rotation is thought to be progressively poorer as one approaches the plasmapause [11]. An indication of the departure from co-rotation is given in Figure 2 by the black dots which portray hypothetical time marks in the equatorial movement of thermal plasma. If one traces the cycle of rotation between $L = 3$ and $L = 4$, it is found that there is a substantial slowing of plasma motion in the bulge region; i.e., a westward drift of ionization is present in the ionosphere as the field tubes are influenced by the convective electric field. At lower latitudes such an effect is absent during magnetically undisturbed times and a more perfect co-rotation is achieved.

Diurnal changes in the F_2 -region produce flows of thermal plasma within the plasmasphere. In addition, the presence of an afternoon bulge in the equatorial plasma profile indicates that significant changes occur in the volume of the plasmaspheric magnetic flux tubes. In the sunlit sectors these volume changes are primarily expansions with a consequent cooling of the plasma and the establishment of an upward refilling plasma flow from the ionosphere. At night the opposite effect occurs. The volume decreases, the plasma is heated, and H^+ is forced out both ends of the field tube into the nighttime F_2 -region.

With the foregoing ideas providing a conceptual framework, it is possible to study a wide variety of experimental data to provide a quantitative verification. Each of the following sections is devoted to a particular aspect of thermal plasma behavior.

Effects of H^+ Flow

A brief description of the chemical processes affecting the formation and loss of H^+ and O^+ in the topside ionosphere was given in the last section. Although the idea of chemical equilibrium at low altitudes matched by diffusive equilibrium above is a convenient concept, it bears little relationship to the actual flow conditions present as a consequence of ionization exchange between the ionosphere and magnetosphere.

The basic equations needed to describe the altitude distribution of O^+ and H^+ have been given elsewhere [12]. Results of ion composition computations based on a realistic model of the topside ionosphere are shown in Figure 3. At low altitudes chemical equilibrium is assumed present. Owing to the increase in the ratio $n(H)/n(O)$ with altitude, the H^+ density also rises rapidly. To introduce the possibility of H^+ flow, H^+ density profiles are shown for four values of the H^+ density at 3000 km; i.e., 10^3 , 5×10^3 , 8×10^3 , 9×10^3 , and 1.5×10^4 ions/cm³. Each of these H^+ boundary densities corresponds to a different H^+ flux, the values for the given boundary densities ranging from 1.35×10^8 ions/cm²/sec for the low H^+ density to -2.3×10^8 ions/cm²/sec for the high H^+ density. Since a negative flux corresponds to plasma inflow, the rightmost profile in Figure 3 is typical of a field tube which supplies the ionosphere with H^+ and, through charge exchange, O^+ . In a similar manner, the lowest H^+ densities are reached when H^+ flows out of the ionosphere. The condition

of diffusive equilibrium is not shown, but lies between the two closely spaced profiles. The fact that the H^+ flux changes from 2.5×10^7 ions/cm²/sec to -2.1×10^6 ions/cm²/sec for a 12% change in the H^+ boundary density gives an indication of the sensitivity of the ionization flux to the high altitude H^+ density.

With regard to the O^+ density, a range of values is obtained which depends upon the H^+ profile. The most rapid decrease of O^+ density with altitude in Figure 3 is associated with the highest density H^+ profile. Likewise, the least rapid decrease of O^+ density with altitude is found for the low density H^+ profile. Such a behavior relates directly to the magnitude of the gravitational induced charge separation electric field acting parallel to \vec{B} . When H^+ is the dominant ion, this electric field is small and O^+ , as a minor constituent, receives little support so its density decreases rapidly with altitude. When H^+ is a minor constituent, a large charge separation field is present and the O^+ density falls off slowly with altitude.

For many purposes the interchange of ionization between the ionosphere and magnetosphere is best described in terms of the reservoir model given in the last section. Within the plasmasphere, field tubes daily expand and contract under the influence of electric fields, thereby inducing continual ionization flow. The magnitude of the H^+ flux associated with changes in the reservoir (3000 km) density is illustrated in Figure 4 using the same ionospheric model shown in Figure 3. In this model the H^+ density at 3000 km is greater than 9×10^3 ions/cm³ plasma flows into the ionosphere, while for smaller densities an outflow occurs. The extreme sensitivity of the inflow flux to reservoir density is apparent.

A different behavior is found as the H^+ boundary density is lowered since the H^+ outflow rapidly approaches a limiting flux such that large decreases in density produce no change in flux. Such a situation is not related to the subsonic or supersonic nature of the flow (the density profiles of Figure 3 correspond to subsonic flow) but depends upon the rate of H^+ diffusion through O^+ (the barrier effect) and the rate of H^+ production via reaction (1) [13].

Since changes in the H^+ reservoir density affect the H^+ flux, it is to be expected that changes in the ionospheric F_2 -region O^+ density at 500 km will produce similar effects. To illustrate this, Figure 5 shows the variation in H^+ flux when the 3000 km H^+ density is held fixed at 10^3 ions/cm³ while the 500 km O^+ density is changed. Diffusive equilibrium for the coupled H^+/O^+ system occurs when the O^+ density is about 5×10^4 ions/cm³. If the O^+ density is larger than this value, there will be an outflow of H^+ , while a smaller value leads to an inward flow. Results such as these are clearly important to the question of the nighttime maintenance of the F_2 -layer [14].

An important aeronautical aspect of thermal plasma flow relates to the density of the neutral hydrogen needed to produce any H^+ flow. The dependence of the H^+ flux on this parameter is shown in Figure 6 where three neutral hydrogen densities have been used with the previous O^+ boundary value of 1.38×10^5 ions/cm³ at 500 km. As hydrogen becomes less abundant, the diffusive equilibrium H^+ boundary density diminishes. As predicted by theory, the limiting H^+ flux is found to be directly proportional to the neutral hydrogen density [13]. Since 7×10^4 atoms/cm³ is not atypical of the hydrogen concentration for moderate solar activity, it appears that the rate of plasma flow will have a significant variation between solar minimum and solar maximum conditions. An example of the short term changes in neutral hydrogen density has recently been given by Mayr and Brinton [15].

The altitude distribution of H^+ depends strongly upon its flow speed relative to O^+ and the relative H^+/O^+ density ratio. Examination of Figure 3 shows that once H^+ is the dominant ion there is no apparent difference between the inward or outward flowing solutions. Such a result follows from the basic equation of motion for H^+ and helps to explain why density distributions which seem to be representative of diffusive equilibrium can actually correspond to substantial ionization transport.

To show this, the steady state H^+ momentum equation can be written as

$$u \frac{du}{ds} + \frac{1}{n} \frac{dp}{ds} + \frac{1}{n_e m} \frac{dp_e}{ds} + g_{||} = -\nu u \quad (3)$$

where u is the transport parallel to \vec{B} , s is a coordinate along \vec{B} , n and n_e are the H^+ and electron densities, m is the H^+ mass, $p = n k T_i$ and $p_e = n_e k T_e$ are the H^+ and electron gas pressures, $g_{||}$ is the parallel component of gravity, ν is the H^+/O^+ transport collision frequency, and the O^+ is assumed stationary.

Consider the high altitude case where H^+ is the dominant ion; i.e., $n = n_e$. Equation (3) gives

$$u \frac{du}{ds} + \frac{1}{n} \frac{dp}{ds} + g_{||} = -\nu u \quad (4)$$

where $p_p = p_e + p$.

When H^+ is the dominant ion far above the F_2 -layer, the term νu of (4) is normally very small. If the flow is such that the term $u du/ds$ is small, (4) can be written as

$$\frac{1}{n_e m} \frac{dp_s}{ds} + g_{||} = 0, \quad (5)$$

precisely the distribution attributed to diffusive equilibrium, even though u itself may be large and of either sign.

Another feature of (5) involves the importance of thermal gradients in determining the actual density profile. Letting $T_p = T_e + T_i$, (5) can be written as

$$\frac{1}{n_e} \frac{dn_e}{ds} + \frac{mg_{||}}{kT_p} + \frac{1}{T_p} \frac{dT_p}{ds} = 0 \quad (6)$$

so that when $dT_p/ds \geq mg_{||}/k$ thermal gradients, rather than gravity will determine the altitude variation of the H^+ density. For mid-latitudes, thermal gradients greater than $0.5^\circ K/km$ will significantly affect the H^+ altitude distribution, a positive gradient reducing the density more rapidly with altitude than would gravity acting alone.

Thermal Plasma in the Plasmasphere

The diurnal exchange of plasma between the topside ionosphere and plasmasphere has been indirectly measured by incoherent scatter radars at Millstone Hill, Massachusetts and Arecibo, Puerto Rico [16]. The Millstone Hill results show large inward and outward flows on the order 10^8 ions/cm²/sec during magnetically quiet periods; i.e., when the plasmasphere is probably in a steady state condition.

The conditions establishing the diurnal flow are found both within the ionosphere and the magnetosphere. Even if there were a strict co-rotation of the plasmasphere, the changes in F_2 -region density and pressure are large enough to drive large H^+ flows in the high altitude regions. For example, between 0600 LT and 1200 LT it is not uncommon for the O^+ density at 500 km to increase by a factor of five or more. Referring to Figure 5, such an increase leads immediately to the flux limited flow of H^+ which, owing to the large volume of mid-latitude magnetic flux tubes, cannot greatly affect the 3000 km

reservoir boundary density for a long period of time. (If 10^8 ions/cm²/sec flow into a volume of 10^{10} cm³, a period of 10^3 sec is needed to increase the H^+ density from 10^3 ions/cm³ to 2×10^3 ions/cm³.) This implies that for this simple model the plasma density of the plasmasphere is determined by the relatively long filling time and should not change greatly from day to day since any surplus reservoir density will be lost very rapidly (there is no limit to the rate of inward flow).

Although such a simple model is useful conceptually, it does not adequately describe the actual variations known to exist within the plasmasphere. To begin with, the F_2 -region undergoes continual variations which are related to the presence of thermospheric winds. Since these changes are of a somewhat irregular nature, the ionization of the plasmasphere must undergo a continual agitation with the presence of compression and rarefaction waves.

Perhaps a more serious variation is related to transverse electric fields having their origin in the mid-latitude dynamo system [17] and the partial penetration of the magnetospheric convection electric field into the outer plasmasphere [18]. The dynamo electric field is established in the lower thermosphere by the flow of neutral winds driven by solar heating of the neutral atmosphere. Theoretical studies have shown that the electric fields established by the dynamo system result in certain regular $\vec{E} \times \vec{B}$ drifts which prevent a strict co-rotation of the high altitude plasma. Typical values of E_1 are of the order 1 to 5 m volt/m can give ionospheric plasma drifts as large as 100 m/sec. Such drifts, if directed towards the magnetic poles, imply changes in the volume of the magnetospheric magnetic flux tubes and a redistribution of enclosed plasma; i.e., flow between the ionosphere and the plasmasphere.

A more important effect of the same type arises from the partial penetration of the convection electric field discussed in the first section. Referring to Figure 2, magnetic flux tubes between $L = 3$ and $L = 4$ tend to be slower than co-rotation in the afternoon bulge region and faster in the morning sector. In addition, field tubes in this same region have simultaneous changes in L value which can greatly alter the total volume. For example, a field tube at $L = 4$ in the morning sector may expand to $L = 6$ in the bulge region. (A schematic sketch of this effect is shown in Figure 7.) Since volume $\propto L^4$, there is a five fold increase in volume, a similar decrease in ion density, and, if the relation PV^Y holds, a factor of 15 decrease in the total plasma pressure. Such a change in the plasmasphere pressure must lead to a replenishment flow of H^+ with a consequent decrease in H^+ density in the topside transition region; i.e., the flow conditions of Figure 3 apply.

In the nighttime an analogous compression of high altitude plasma must occur with there being a large increase in plasma density and pressure as the field tubes drift from $L = 6$ to $L = 4$. In fact, such a compression of an already dense plasma can lead to a sharper density gradient at the plasmopause than might otherwise be expected.

Although it is convenient to assume that motions of field tubes are accompanied by a very rapid redistribution of the thermal plasma along the field tube, such a process may be sufficiently slow to permit sizeable parallel pressure gradients to exist. In the nightside compression, for example, there is a differential effect which tends to compress the plasma more strongly in the equatorial region than at other points along the same field tube. This creates a positive pressure gradient which drives an initial flow towards the earth at speeds of 1 to 10 km/sec.

It is clear from the foregoing discussion that drift motions across L shells will drive plasma into or out of the plasmasphere. While the inward flow rate has no theoretical limit, the outflow does and in this situation the O^+ to H^+ transition moves upwards to great heights (see Figure 3).

Effects of Magnetic Disturbances

Observations of the location of the plasmopause show a strong dependence upon

magnetic activity [19]. This variation is clearly shown in Figure 8, taken from the work of Chappell et al. [9] and based onOGO-Y thermal ion measurements in the night-time regions. In essence, increases in the level of magnetic activity move the plasmapause to lower latitudes through an intensification of the convection electric field. The thermal ionization in the newly exposed field tubes is rapidly swept away and an upward flow of H^+ from the ionosphere immediately begins; i.e., the polar wind is established to the new plasmapause.

As magnetic activity declines, the convective electric field weakens such that plasma is no longer swept away to the magnetopause over the region previously exposed. In other terms, the field tubes once again co-rotate with the earth and are subject to the diurnal ebb and flow effects. However, since virtually all plasma in the field tube was lost during the disturbance, a long period of refilling must follow before a steady state is reached. In the initial refilling period the thermal plasma density is sufficiently low that the upward H^+ flux is supersonic [20]. This implies the formation of a shock travelling down the field tube and an eventual transition to subsonic flow. The upward flux of ionization is unaffected by these matters, however, and continues at its flux limited value until nearly steady state conditions are reached.

Observations of the refilling process have been made [21] using the characteristics of radio whistlers. Owing to the relatively slow rate of refilling, it appears that 5 to 8 days are required to replenish the emptied mid-latitude field tubes. Since magnetic disturbances tend to occur more frequently than this, the plasmasphere recovery from one storm may not be completed before another cycle starts. This would tend to keep the exposed regions in continual flow and reduce the plasma density below equilibrium values.

Another aspect of magnetic storms is the way in which the high altitude plasma of the old plasmasphere is lost. On the dayside of the earth a stronger convective field results in a drift of plasma towards the magnetopause (towards high latitudes in the ionosphere). This is equivalent to a reduction in plasma pressure and the ionosphere responds with an upward H^+ replenishment flow. On the nightside there is a tendency to compress the plasmasphere towards the earth; i.e., plasma is moved inwards to lower L values and lost through parallel flow through the feet of field tubes to the upper F_2 -region. This flow will enhance the F_2 -layer density and move the peak to a higher altitude. Again, it must be realized that there is a clear relationship between cross L shell movements of ionospheric plasma and an associated flow of plasma along the lines of magnetic force.

Thermal Plasma Behavior at High Latitudes

Several recent reviews have been given of the conditions affecting the topside thermal plasma in those regions of the earth lying outside the plasmasphere [22]. Owing to the presence of the convection electric field plasma is continually swept away from the earth in the direction of the front of the magnetopause (see Figure 2). This sweeping effect is responsible for electron and ion pressure gradients directed along the magnetic field lines. This, in turn, establishes an upward flow of H^+ whose source, given by (1), lies in the upper F_2 -region. Because the sweeping action of the $\vec{E} \times \vec{B}$ drift is rapid, the plasma densities within the magnetosphere are low and the ionosphere supplies H^+ at the maximum rate possible with fluxes in the range 7×10^7 to 2×10^8 ions $cm^{-2}sec^{-1}$.

Typical ion density profiles computed for a summer polar cap are shown in Figure 9. The corresponding H^+ velocity, given in Figure 10, indicates that the flow eventually becomes supersonic. Although the term polar wind was originally adopted [23] to describe this supersonic flow for the regions where the geomagnetic field lines connect to the magnetosheath, theory and experiment show that virtually all regions outside the plasmapause have large escape flows of H^+ . As shown previously,

the magnitude of the flux is virtually independent of the supersonic condition. Hence, the term polar wind can be used to describe the general high latitude plasma escape process, even though the flow itself may not be supersonic at a given altitude.

To illustrate the geographical extent of the polar wind, data obtained from Explorer 31 measurements [24] are shown in Figures 11 and 12 to represent summer and winter conditions. Each solid line represents an observation of greater than 1 km/sec H^+ flow, while the dotted lines indicate periods when no flow was seen. The fluxes were found to be of the order 5×10^7 ions/cm²/sec in the summer and 10^8 ions/cm²/sec in the dark winter polar regions. The difference probably arises from a change in neutral hydrogen density associated with different temperatures of the thermosphere.

Independent evidence for the polar wind flow outside the plasmapause has recently been found in high altitude Alouette II electron density profiles. To illustrate, profiles of electron density as a function of invariant latitude are shown for five altitudes in Figure 13. This nighttime pass shows the presence of a sharp plasmapause near 60°A. Inside the plasmasphere the electron density contours are closely spaced, indicating a large electron density scale height and the presence of H^+ in substantial quantity. Poleward of the plasmapause a more erratic behavior is seen with the high altitude variations between 67° and 74°A representing auroral zone heating. Even in this region, however, the electron density contours give plasma scale heights of the order of 400 to 600 km; i.e., typical of O^+ alone. Detailed analysis of records such as these has shown that the presence of O^+ to 2500 km can be explained only if the neutral hydrogen density is very low; i.e., much less than 10^4 cm⁻³, or if there is a polar wind flow of H^+ with a flux in the range 7×10^7 to 2×10^8 ions/cm²/sec. Since measurements [15] rule out the possibility of the very low neutral hydrogen densities, it must be concluded that the observed behavior is a consequence of H^+ flow. Another example of this behavior at high latitudes is shown in Figure 14.

The schematic trajectory of plasma drift at high latitudes can be obtained from Figure 2 through projection of the dipolar field lines into the ionospheric regions. Figure 15 shows a typical drift pattern at high latitudes including both the plasmapause and the extension of the polar cusp.

Although it is convenient to think of thermal plasma convection in terms of a steady motion, numerous experiments have found that convection is strongest during polar substorms [24]. While the convection patterns seem to be consistent with the original theory of magnetospheric convection, the plasma drift is at times greatly enhanced. To illustrate, Figure 16 shows the results of a 24 hour measurement of plasma drift velocities at Chatanika, Alaska ($L = 5.6$) obtained by incoherent scatter radar. The data, plotted with the geomagnetic pole at the center of the diagram, show that in the late afternoon and early evening the $\vec{E} \times \vec{B}$ flow velocities are small. With the onset of a substorm near 2000 LT a rapid southwesterly drift begins. Near midnight there is a reversal and the flow is almost due east (magnetic). During the rest of the day the flow is generally directed back over the polar cap. Comparison of these results with the schematic flow trajectories of Figure 15 shows many similarities. Thus, at least in these disturbed times it can be concluded that the large scale convective field needed to sweep high altitude plasma to the magnetopause is present. Similar measurements made during periods of low substorm activity have shown that the nighttime enhancement of drift velocities is largely absent and the observed drift velocities remain less than 150 m/sec throughout the day and night. Although it might be thought that the slowness of convective drift would lead to a rapid filling of the polar magnetosphere with thermal H^+ , the time scale for this to happen is of the order of several days, substantially greater than the time between substorms. Consequently, the refilling process is never able to create a substantial H^+ concentration in the topside ionosphere outside the plasmasphere.

As illustrated by Figure 1, two types of field lines lead from the high latitude ionosphere: those connected to the magnetosheath and those forming closed dipole-like loops. When the supersonic polar wind is convected onto a closed field line a shock

front is formed which propagates down the field tube towards the earth. Calculations of the time needed for this shock to reach the ionosphere and convert the flow to subsonic speeds indicate periods of 10 to 20 hours. To illustrate, a plot of plasma density as a function of distance along a convecting magnetic field tube is shown in Figure 17. Although shock transition moves towards the earth rapidly at first, it eventually slows so that the actual transition to subsonic flow takes an extended period of time. Since the upward plasma flux is unaffected by this transition, it appears that the polar wind flow must continue as a general feature for both disturbed and undisturbed conditions. [25]

Future Studies

Our knowledge of thermal plasma behavior in the magnetosphere is based on a relatively small number of experiments. Many important phenomena thought to exist; i.e., reconnection shocks, flow of plasma in field tubes, and plasma compression and rarefaction have yet to be confirmed. Nevertheless, it is clear that the thermal plasma of the topside ionosphere is not quiescent and must undergo a wide variety of motions consistent with changes in the underlying ionosphere and the surrounding magnetosphere.

Within the plasmasphere the most important study relates to the validity of the plasma reservoir concept; i.e., are cross-L drifts of plasma accompanied by inward or outward (parallel to \vec{B}) flows?

Although many studies assume a diffusive type density distribution of plasma along lines of magnetic force, proper measurements have never been made and the actual density profile may show pressure gradients associated with shock fronts or compression and rarefaction effects.

Outside the plasmasphere virtually no magnetospheric thermal plasma measurements have been made to determine parallel flow speeds, temperatures, or ion flux.

In many respects theory leads experiment in the investigation of thermal plasma behavior. Before further significant progress can be made it will be necessary to obtain a better idea of the actual physical conditions present in the various regions of the magnetosphere.

References

- [1] Storey, L. R. O., Phil. Trans. Roy. Soc., 246A, 113 (1953).
- [2] Dungey, J. W., in The Physics of the Ionosphere, The Physical Society, London p. 406 (1955).
- [3] Johnson, F. S., J. Geophys. Res., 65, 585 (1960).
- [4] Gringauz, K. I., Planet. Space Sci., 11, 281 (1963).
- [5] Carpenter, D. L., J. Geophys. Res., 68, 1675 (1963).
- [6] For a historical review, see Axford, W. I., Rev. Geophys., 7, 421 (1969).
- [7] Mayr, H. G., J. M. Grebowsky, and H. A. Taylor, Planet. Space Sci., 18, 1123 (1970).
Park, C. G., J. Geophys. Res., 75, 4249 (1970).
Hoffman, J. H., Trans. Am. Geophys. Union, 49, 253 (1968).
Carpenter, D. L., J. Geophys. Res., 71, 693 (1966).
- [8] Banks, P. M. and T. E. Holzer, J. Geophys. Res., 74, 6317 (1969).
Banks, P. M., A. F. Nagy and W. I. Axford, Planet. Space Sci., 19, 1053 (1971).
- [9] Chappell, C. R., K. K. Harris and G. W. Sharp, J. Geophys. Res., 75, 50 (1970).
Harris, K. K., G. W. Sharp and C. R. Chappell, J. Geophys. Res., 75, 219 (1970).
- [10] Fehsenfeld, F. C. and E. E. Ferguson, J. Chem. Phys., 55, 2120 (1971).
- [11] Chappell, C. R., K. K. Harris and G. W. Sharp, J. Geophys. Res., 75, 3848 (1970).
- [12] Hanson, W. B. and T. N. L. Patterson, Planet. Space Sci., 12, 979 (1964).
Banks, P. M. and T. E. Holzer, J. Geophys. Res., 74, 6304 (1969).
Schunk, R. W. and J. C. G. Walker, Planet. Space Sci., 18, 1319 (1970).
- [13] Geisler, J. E., J. Geophys. Res., 72, 81 (1967).
- [14] Hanson, W. B. and I. B. Ortenburger, J. Geophys. Res., 66, 1425 (1961).
Hanson, W. B. and T. N. L. Patterson, Planet. Space Sci., 12, 979 (1964).
- [15] Mayr, H. G. and H. C. Brinton, J. Geophys. Res., 76, 3738 (1971).
- [16] Evans, J. V., Radio Sci., 6, 843 (1971).
Evans, J. V., Radio Sci., 6, 855 (1971).
Ho, M. C. and D. R. Moorcroft, Planet. Space Sci., 19, 1441 (1971).
- [17] Matsushita, S., Radio Sci., 6, 279 (1971).
Matsushita, S. and J. D. Tarpley, J. Geophys. Res., 75, 5433 (1970).

- [18] Brice, N. M., J. Geophys. Res., 72, 5193 (1967).
 Kavanagh, L. D., J. W. Freeman and A. J. Chen, J. Geophys. Res., 73, 5511 (1971).
 Nishida, A., J. Geophys. Res., 71, 5669 (1966).
- [19] Rycroft, M. J. and S. J. Burnell, J. Geophys. Res., 75, 5600 (1970).
 Chappell, C. R., K. K. Harris and G. W. Sharp, J. Geophys. Res., 75, 50 (1970).
- [20] Banks, P. M., A. F. Nagy and W. I. Axford, Planet. Space Sci., 19, 1053 (1971).
 Carpenter, D. L., J. Geophys. Res., 75, 3837 (1970).
- [21] Park, C. G. and D. L. Carpenter, J. Geophys. Res., 75, 3825 (1970).
- [22] Banks, P. M. in Physics of the Polar Magnetosphere, K. Folkestad, editor, University of Oslo Press, Oslo, p. 75 (1972).
- [23] Axford, W. I., J. Geophys. Res., 73, 6855 (1968).
 Banks, P. M. and T. E. Holzer, J. Geophys. Res., 73, 6846 (1968).
- [24] Doupnik, J. R., P. M. Banks, M. J. Baron, C. L. Rino, and J. Petriceks, J. Geophys. Res., (to appear, 1972).
 Mozer, F. S. and R. H. Manka, J. Geophys. Res., 76, 1697 (1971).
 Carpenter, D. L. and K. Stone, Planet. Space Sci., 15, 395 (1967).
 Wescott, E. M., J. D. Stolarik and J. P. Heppner, J. Geophys. Res., 74, 3469 (1969).
 Akasofu, S. I., Space Sci. Rev., 4, 498 (1965).
- [25] Grebowsky, J. M., Model Development of Supersonic Trough Wind with Shocks, NASA Report X-621-72-53. Goddard Space Flight Center, February (1972).

Captions

- Figure 1. Model of the Earth's Plasma and Magnetic Field Environment. The dark arrows indicate polar wind ion flow outside the plasmasphere. Similar flows sometimes present inside this region are not shown.
- Figure 2. Plasma Drift Motions Viewed in the Magnetic Equatorial Plane. Outside the plasmapause the convection pattern lead to a loss of thermal plasma at the magnetopause. Inside the plasmasphere co-rotation effects are most important. The relative speed of this plasma is indicated by the black dots. Because the magnetic field is of a dipole nature, there is a considerable change in field tube volume implied in all cross - L motions.
- Figure 3. Topside Ion Composition with H^+ Flow Effects. The model is based on a $1000^\circ K$ model thermosphere and an O^+ density of 1.38×10^5 ions/cm³ at 500 km. Chemical equilibrium is assumed at 500 km and H^+ flow is obtained by varying the H^+ density at 3000 km. The numbers above each profile give the H^+ flux at 3000 km. A positive flux corresponds to upward flow. A neutral hydrogen density of 1.92×10^5 /cm³ was chosen at 500 km.
- Figure 4. H^+ flux for Different H^+ 3000 km Boundary Densities. The fluxes of Figure 3 are plotted as a function of the H^+ boundary density. Diffusive equilibrium corresponds to zero flux. Large H^+ inflow follows for relatively small increases of density. The H^+ outflow has a limiting value.
- Figure 5. Variation of H^+ Flux with O^+ Boundary Density. The H^+ density at 3000 km is fixed at 10^3 ions/cm³ and the 500 km O^+ density is varied. Diffusive equilibrium for H^+ occurs at $n(O^+) = 5.5 \times 10^4$ ions/cm³. Smaller values lead to large inflow while the outflow increases gradually as larger values are chosen.
- Figure 6. Variation of H^+ Flux with Neutral Hydrogen Density. The model given in Figure 3 was used with different neutral hydrogen densities. Both the limiting flux and the equilibrium H^+ density are affected by these changes.
- Figure 7. Schematic Variation of Magnetic Flux Tube Volume. As field tubes move across L-shells their volume changes as Volume $\propto L^4$. Plasma redistributions are brought about by pressure gradients which move plasma along the field tube.
- Figure 8. Location of the Plasmapause. Experimental OGO-V results showing the location of the plasmapause for different levels of magnetic activity.

- Figure 9. High Latitude Ion Composition Profiles. Theoretical models were used to compute the ion composition for the polar regions. The flow becomes supersonic above 4100 km. The large H^+ flux is a consequence of a slightly high neutral hydrogen density and a large O^+ density (see Figure 5).
- Figure 10. Profiles of High Latitude H^+ Velocity. The profiles are given for three model neutral atmospheres and identical F_2 -region photoionization rates. The crosses indicate the point of transition to supersonic flow.
- Figure 11. Experimental Observation of Summer H^+ Flow from Explorer 31. The arrows indicate portions of the satellite path when data was obtained. Dotted arrows are plotted for times when no flow was seen (< 1 km/sec). The extent of the solid arrows support the idea of plasma flow in all areas outside the plasmasphere.
- Figure 12. Experimental Observation of Winter H^+ Flow from Explorer 31. Owing to the very low plasma densities relatively fewer observations were possible. Nevertheless, the ion flow was found in the expected regions outside the plasmasphere.
- Figure 13. Observations of High Latitude Electron Densities from Alouette II. The topside radio sounder provided altitude profiles of electron density. These summertime plots show contours of electron density as a function of invariant latitude in the midnight sector. The plasmopause is seen in the topside near $60^\circ A$ while auroral zone heating centers at $70^\circ A$. The contours indicate only O^+ outside the plasmopause; i.e., a polar wind flow is present.
- Figure 14. Observations of Summer High Latitude Electron Densities from the Alouette II Sounder. The lack of significant variations is typical of the daytime topside ionosphere outside the plasmopause. The plasma scale height indicates the presence of O^+ and an H^+ flow of 1.5×10^8 ions/cm²/sec can be inferred.
- Figure 15. Plasma Drift Motion Outside the Plasmasphere. The closed curves give the trajectories of plasma motion obtained from projecting the equatorial drifts of Figure 2 into the ionosphere. The shaded area corresponds regions where the magnetic field lines connect to the magnetosheath. Measurements show that the speed of motion varies greatly with highest velocities being seen during polar substorms.
- Figure 16. Observations of Plasma Convection. These data represent the observed plasma velocities at Chatanika, Alaska ($L = 5.6$) on February 11-12, 1972 at an altitude of 163 km. The dial gives local time and directions are related to magnetic north at the center. A substorm is believed to have started near 2200 LT and continued through 0400 LT. The overall behavior agrees in many respects with the model shown in Figure 15.

Figure 17. Reconnection Shock Front Motions. A model of plasma flow along an $L = 6$ field tube has been used to give the downward motion of the shock front which attempts to convert the supersonic polar wind to subsonic speeds [25]. The shock starts at the magnetic equator and slowly moves towards the earth. Because convection of the field tube is faster than the shock motion a transition to subsonic flow probably does not occur. The H^+ flux is the same in either case, however.

DISCUSSION

Martelli: Could you expand on the assumptions you have used for your theoretical model? In particular, what expression for the pressure (scalar? tensor?) have you used, and what stability criteria for the highly energetic fluxes?

Banks: The basic equations are given in a recent paper (Planetary and Space Science 19, 1053, 1971). We assume a scalar pressure and ignore the presence of energetic particles. Changes in the effective H^+/O^+ collision frequency do not greatly affect the H^+ flux but do alter the H^+ density profile.

Hasegawa: What effect does the convective loss of plasmopause particles have on the dynamics of filling a flux tube?

Banks: It is just the convective loss which maintains a low plasma pressure along a field tube, thereby inducing upward flow.

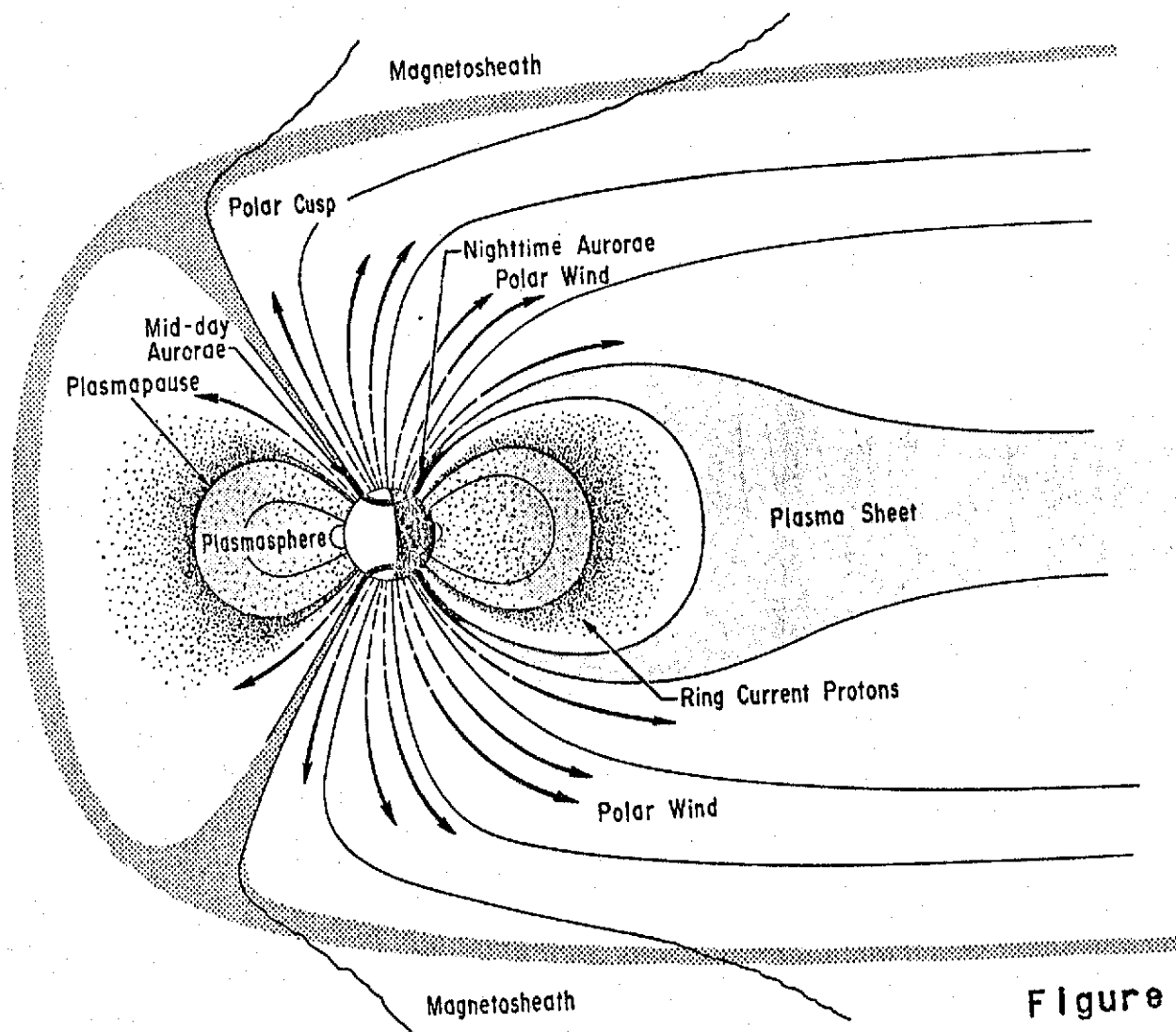


Figure 1

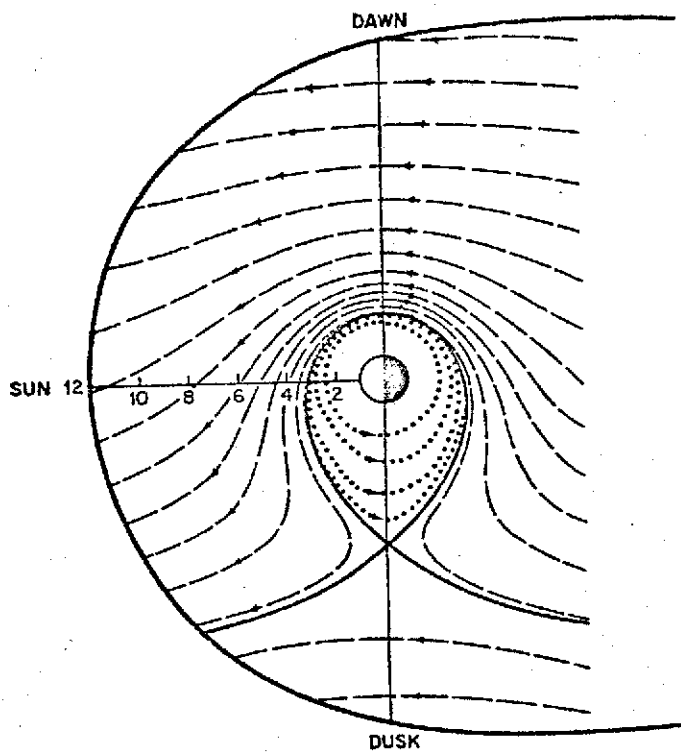


Figure 2

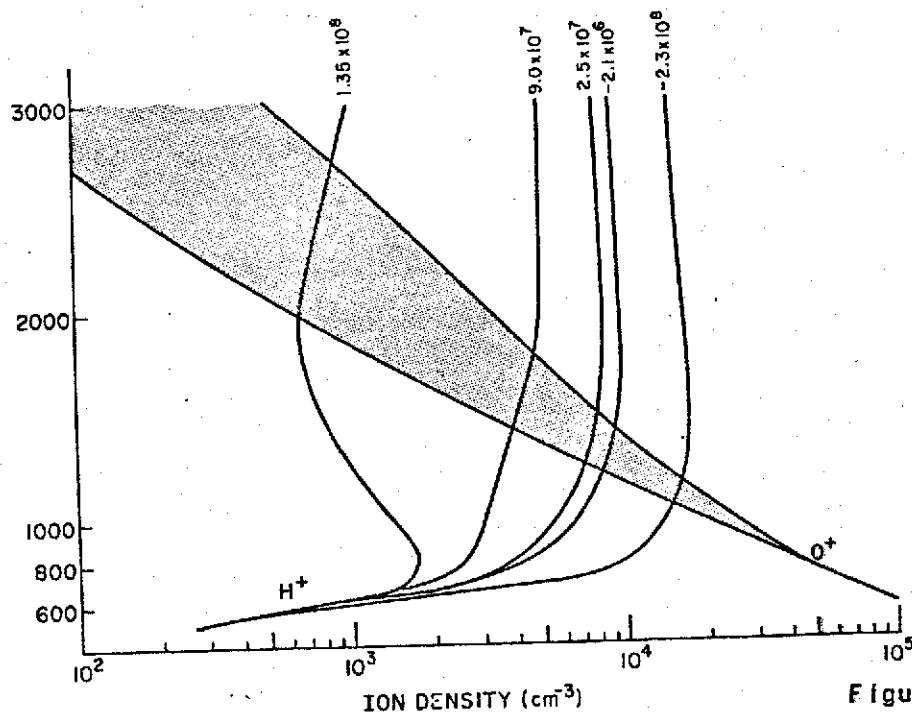


Figure 3

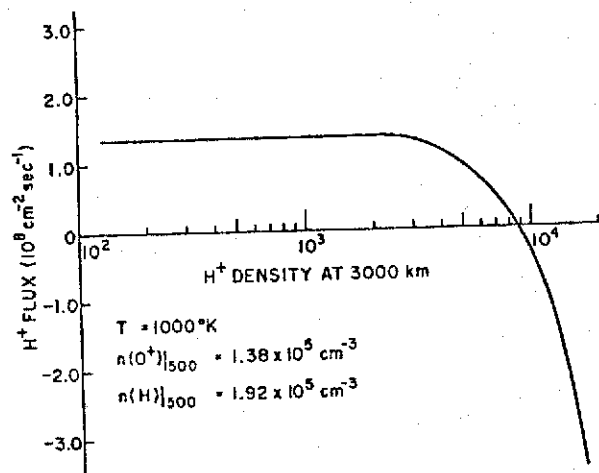


Figure 4

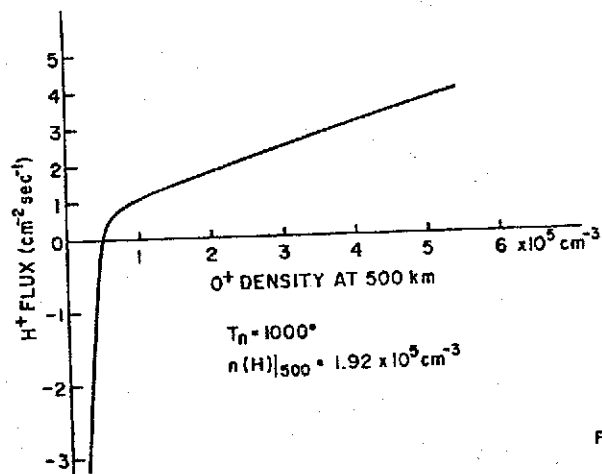


Figure 5

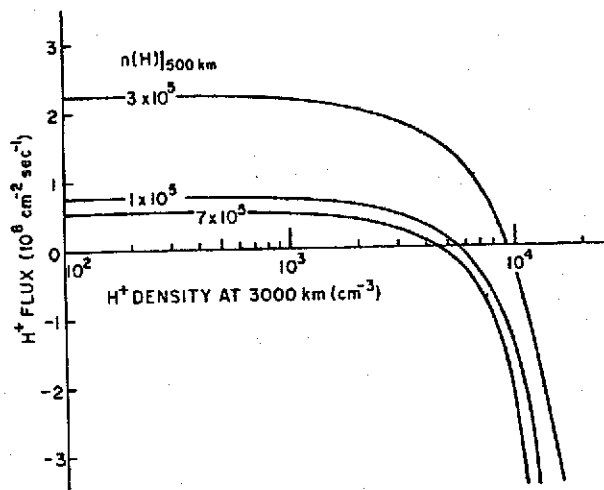


Figure 6

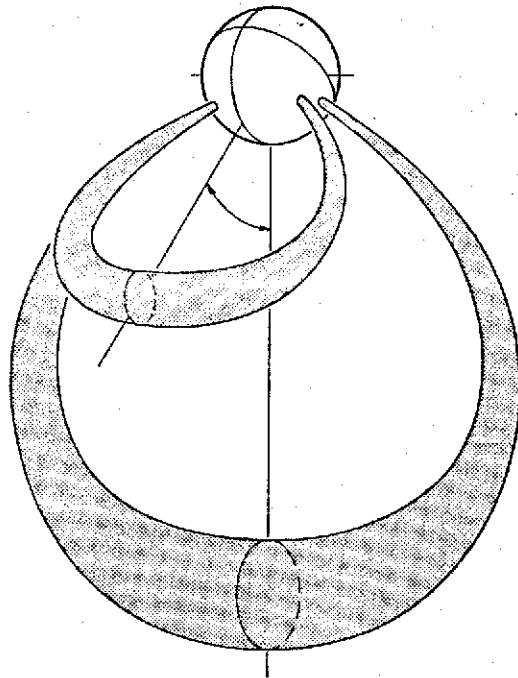


Figure 7

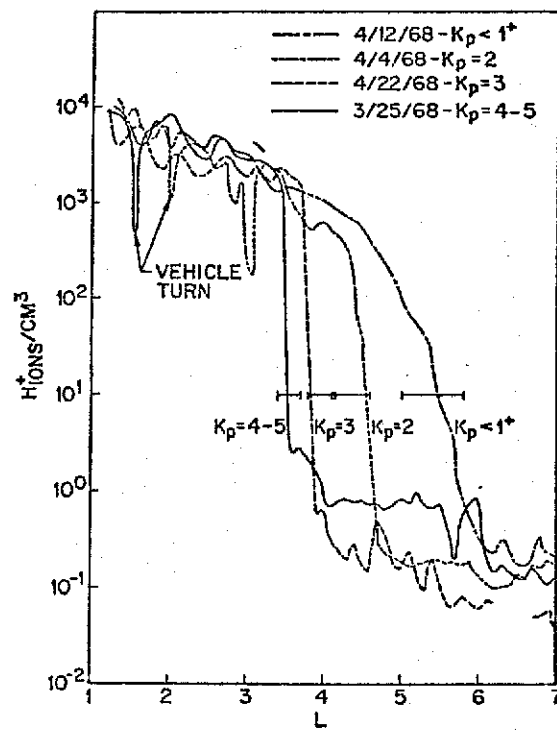
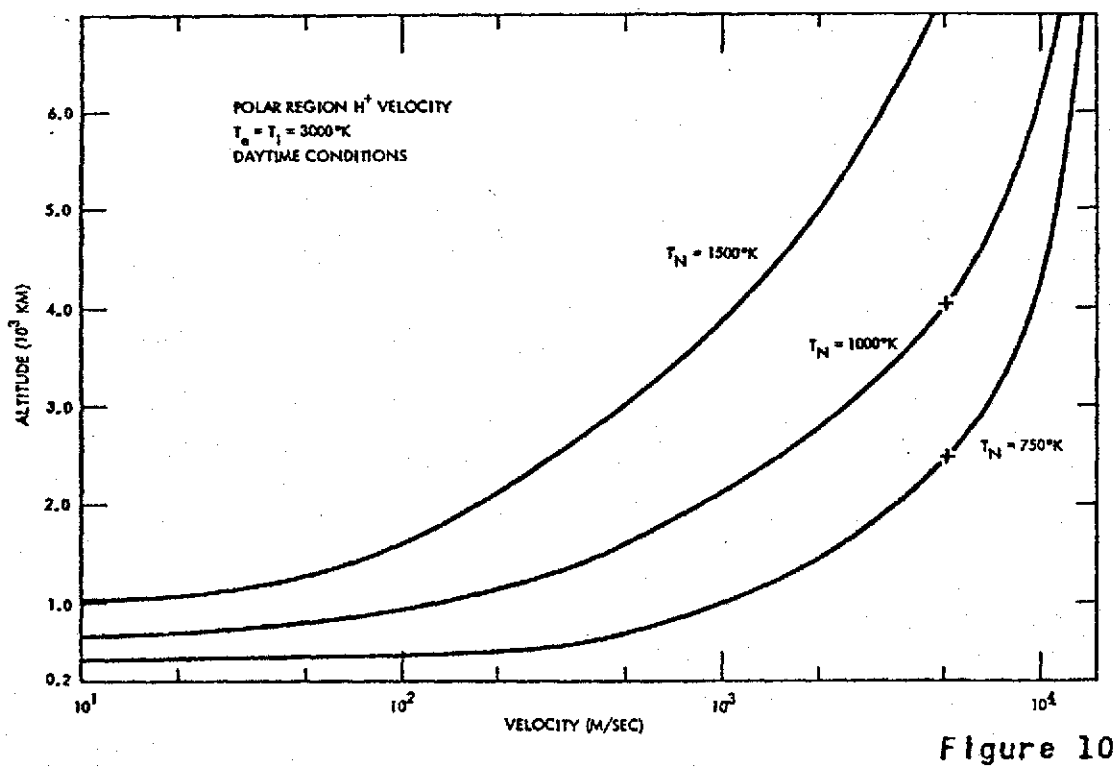
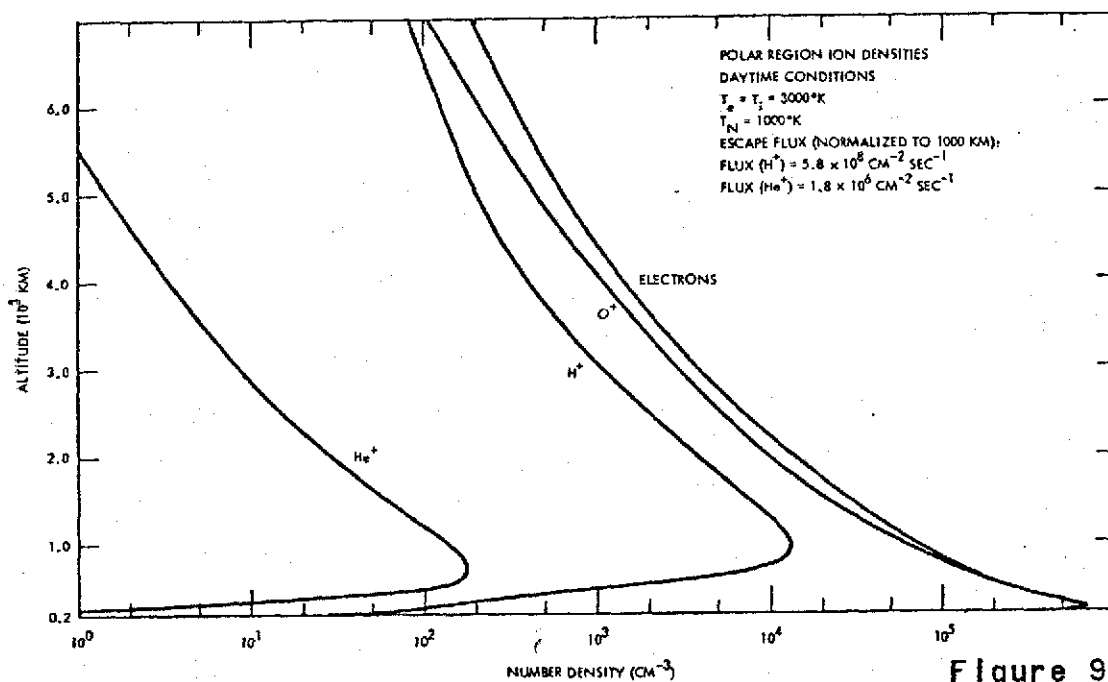


Figure 8



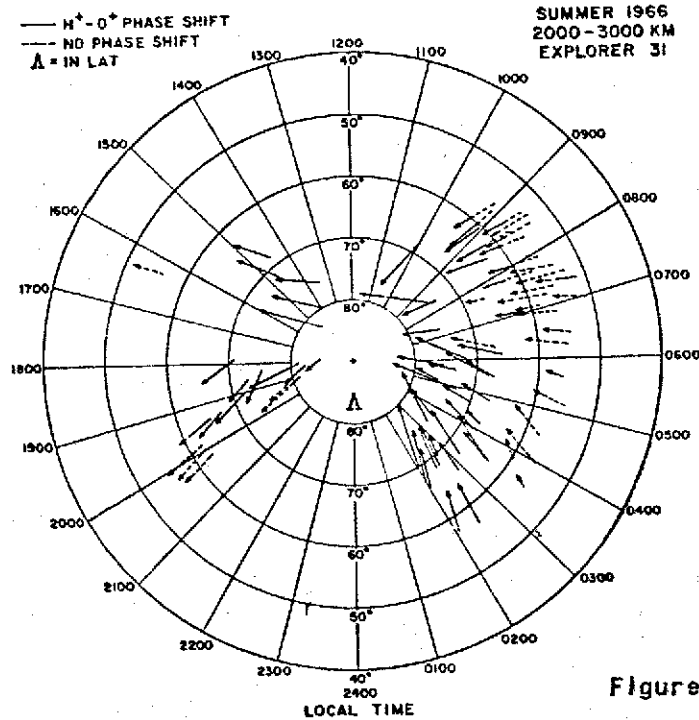


Figure 11

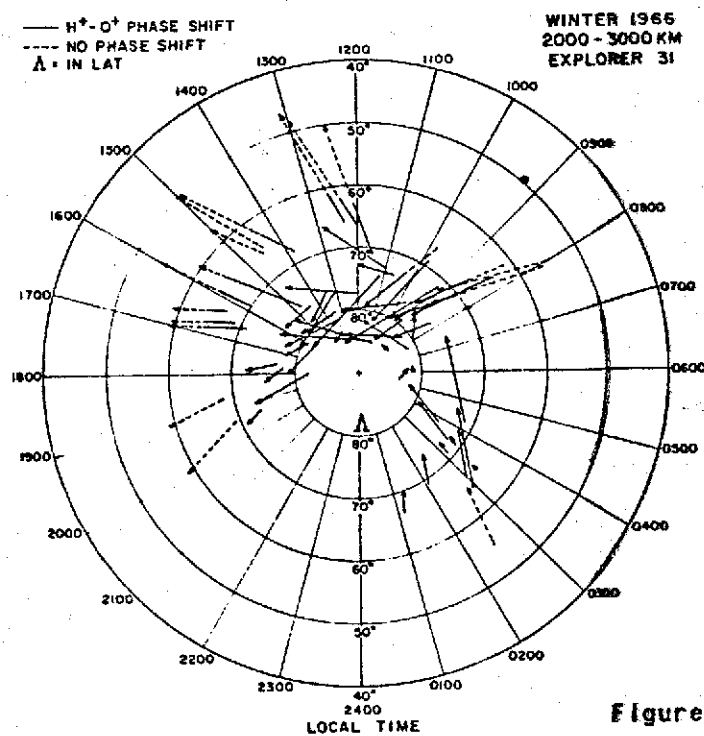
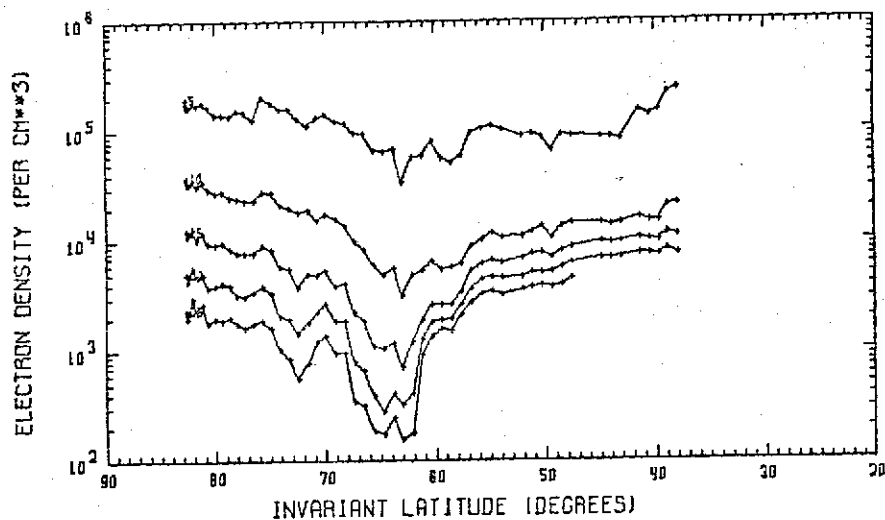


Figure 12

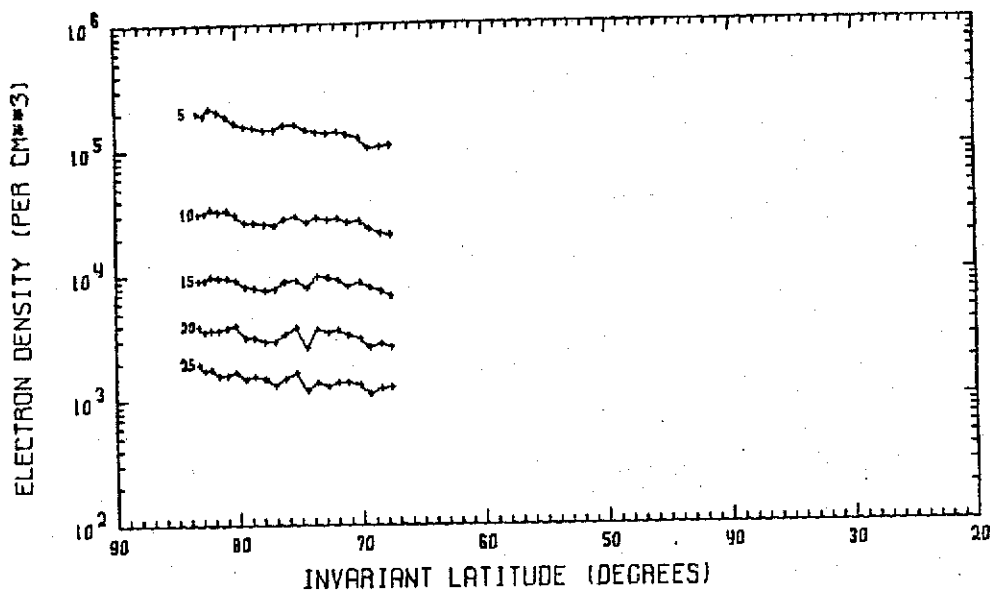


DATE(DMY) 26 7 68 START TIMES UT= 0650 LT= 2317

STATION OTTA

KP= 2

Figure 13



DATE(DMY) 8 7 68 START TIMES UT= 0831 LT= 0202

STATION OTTA

KP= 2-

Figure 14

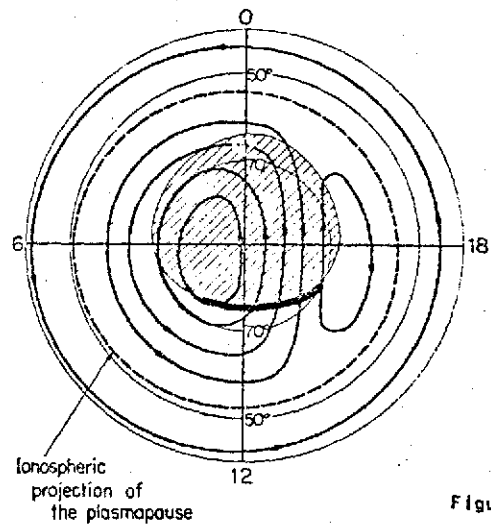


Figure 15

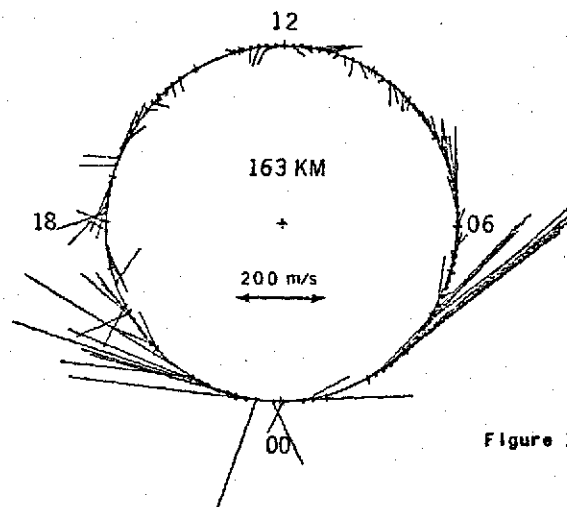


Figure 16

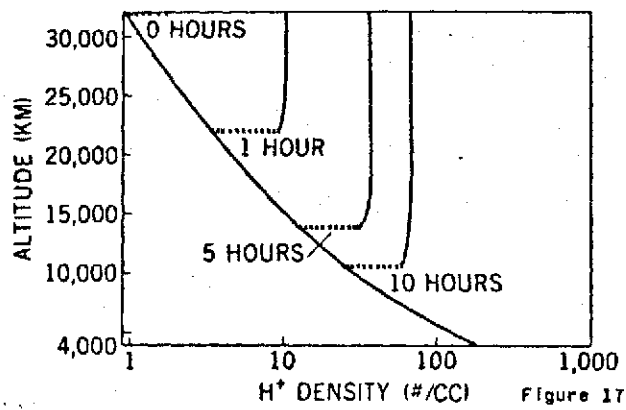


Figure 17

P.A.S.S.
1st Proof
The Universities Press, Belfast

315
MS pages 1-27

Pergamon Press, Oxford
Galileys 1-8
28.9.73

1

Planet. Space Sci. 1973, Vol. 21, pp. 315 to 331. Pergamon Press. Printed in Northern Ireland

THERMAL PROTON FLOW IN THE PLASMASPHERE: THE MORNING SECTOR

PETER M. BANKS*

Radioscience Laboratory, Stanford University, Stanford, California 94305, U.S.A.

and

JOE R. DOUPNIK

Department of Applied Physics and Information Science, University of California,
San Diego, La Jolla, California 92037, U.S.A.

(Received 28 May 1973)

Abstract—Vertical profiles of electron density obtained in the vicinity of the plasmapause using the Alouette-II topside sounder have been analyzed to assess the presence of H^+ flow in the topside ionosphere. The observations in the midnight sector show clearly the presence of the plasma-pause; i.e. there is a sharp boundary separating the poleward regions of polar wind H^+ flow and the more gentle conditions of the plasmasphere where light ions are present in abundance. In contrast, in the sunlit morning sector upwards H^+ flow is deduced to be present to invariant latitudes as low as $43^\circ (L = 2.2)$ in the regions normally known to be well inside the plasma-sphere. The upwards H^+ flux is sufficiently large (3×10^3 ions $cm^{-2} sec^{-1}$) that the plasma-pause cannot be seen in the latitudinal electron density contours of the topside ionosphere. The cause for this flow remains unknown but it may be a result of a diurnal refilling process.

1. INTRODUCTION

During the past several years there has been an increasing appreciation of the dynamical coupling between the ionospheric F_2 -region and the magnetosphere. In the regions exterior to the plasmasphere both the O^+ of the F_2 -layer and the H^+ of the topside ionosphere are exposed to the general magnetospheric electric field. As a consequence, thermal plasma in this region undergoes an $\vec{E} \times \vec{B}$ drift which leads to plasma loss at the magnetopause and consequently to the establishment of large scale upward polar wind flows of H^+ .

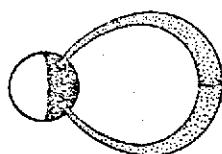
For magnetically quiet conditions, the plasmapause represents the boundary between plasma which attempts to co-rotate with the Earth and plasma which is exposed to the magnetospheric electric field. (A recent review has been given by Chappell, 1972.) Within the plasmasphere the behavior of H^+ and He^+ is governed by ion flow along magnetic field lines in response to changes in plasma pressure and chemical composition. Such changes occur at low latitudes as a result of F_2 -region ionization and thermal processes and at high latitudes as a consequence of $\vec{E} \times \vec{B}$ plasma drift associated with the partial penetration of the magnetospheric convection electric field inside the plasmapause boundary. The effects of the $\vec{E} \times \vec{B}$ drift are especially important in the afternoon and evening sectors of the plasmasphere where plasma motions across field lines normally occur and lead to substantial plasma pressure gradients along the lines of magnetic force.

The idea of diffusive equilibrium between O^+ in the F_2 -region and the light ions of the topside ionosphere has been explored in a number of theoretical studies (Mange, 1960; Kockarts and Nicolet, 1963; Bauer, 1966; Rush and Venkateswaran, 1965). Outside the plasmasphere, however, measurements provide evidence for the existence of a much more dynamic state with high speed flows occurring at high altitudes acting to replenish regions depleted of ionization by $\vec{E} \times \vec{B}$ drifts (Brinton *et al.*, 1971; Hoffman, 1969; Banks,

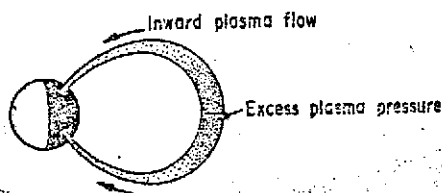
* On leave of absence from the University of California, San Diego, U.S.A.

1972). Theoretical studies of these regions (Banks and Foster, 1969a, Marubashi, 1970; Mayr *et al.*, 1970) have shown the flow to consist principally of H^+ moving at speeds near or greater than the ion thermal speed.

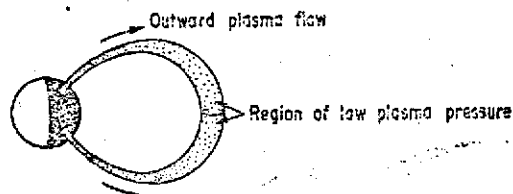
The question of light ion flow within the plasmasphere represents a more difficult problem. To a large extent the thermal plasma of the plasmasphere acts as a fluid contained in a reservoir with flow along field lines resulting from changes in pressure or volume. A schematic view of the reservoir concept with associated plasma flows is shown in Fig. 1. During magnetic storms a large portion of the plasma stored in such magnetic flux tube reservoirs is removed by transverse electric fields, either through sweeping away to the magnetopause (on the dayside) or through compression and subsequent inward flow to the ionosphere (on the nightside) [See Chappell (1972) for a more detailed description and appropriate references]. Following magnetic storms, ionospheric replenishment of the thermal plasma reservoir proceeds via O^+/H charge exchange in the 600-1000 km region and an upward flow of H^+ into the plasmasphere (Park, 1971; Evans, 1971a,b; Banks *et al.*, 1971). Calculations of the thermal plasma behavior for these periods of refilling have shown that far out along the magnetic field tubes the H^+ flow is initially supersonic and becomes subsonic only after a number of hours have elapsed. In either case there is a net outwards H^+ flow for several days.



Diffusive Equilibrium: Static distribution of plasma with small inward flow at low altitudes to accommodate ion losses in the F_2 -region.



Inward Diffusive Flow: Plasma moves inward and is lost in the F_2 -region. Speed of flow may become supersonic if excess plasma pressure is sufficiently large.



Outward Diffusive Flow: Plasma moves outward to equalize plasma pressure. Speed of flow may become supersonic if pressure deficit is large.

FIG. 1. SCHEMATIC VIEW OF COOL PLASMA BEHAVIOR IN THE TOPSIDE IONOSPHERE.

For less is known about the diurnal plasma flow in the absence of refilling effects associated with magnetic storms. Incoherent backscatter observations at Millstone Hill ($L = 3.1$) and Arecibo ($L = 1.9$) have shown the presence of large (10^8 ions $\text{cm}^{-2} \text{sec}^{-1}$) O^+ flows which are believed to be associated, via charge exchange, with H^+ flow into the plasmasphere (Evans, 1971a,b; Ho and Moorcroft, 1972). Theoretical studies based on the equations of continuity and momentum conservation for O^+ and H^+ indicate the presence of large diurnal variations in H^+ flow (and consequently O^+ flow) resulting from changes in temperature and density of the ionosphere (O^+) and of the neutral atmosphere (O and H) [Nagy and Banks, 1972; Schunk and Walker, 1972; Mayr *et al.*, 1972; Moffett and Murphy, 1973; Geisler and Bowhill, 1965; Hanson and Patterson, 1964]. Typical calculated results for the diurnal H^+ flux at Millstone Hill are shown in Fig. 2, taken from Nagy and Banks (1972).

The currently available direct observations of topside plasma flow are relatively sparse and give an incomplete picture of the important latitude and local time effects. As shown in this paper, however, information about H^+ flows can be deduced from electron density profiles obtained using high altitude radio sounders carried by satellites such as ISIS-I and Alouette-II. Such profiles, when interpreted in terms of multi-ion continuity and momentum equations appropriate to the topside ionosphere, can provide important data on the spatial and temporal extent of thermal plasma flow inside and outside the plasmasphere.

In the present study, an analysis of Alouette-II electron density profiles has been made. The results, discussed in detail in later sections of this paper, reveal the existence of a large scale upwards H^+ flow in the morning sector of the plasmasphere extending from the post-sunrise regions into the afternoon sector. In latitude it appears to range from the deep polar cap down to $\Lambda \approx 45^\circ$ invariant latitude. The cause for this flow is unknown, but it could represent either the refilling of flux tubes previously emptied into the night-time F_2 -region or the cross- L drifts of plasma associated with the partial penetration of the convection electric field into the plasmasphere.

The experimental data of this paper are discussed in the next section. The interpretation

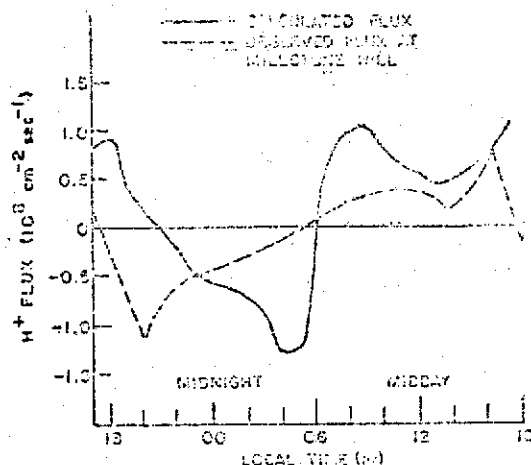


FIG. 2. COMPUTED AND OBSERVED DIURNAL H^+ FLUXES AT MILLSTONE HILL, MASSACHUSETTS FOR 23-24 MARCH 1970.

of the data in terms of multi-ion models is described in Section 3, while Section 4 provides a general discussion of the results.

2. MEASUREMENTS

The Alouette-II satellite includes a sweep frequency ionospheric sounder which permits an accurate determination of electron density as a function of altitude. A complete discussion of the equipment and method of analysis needed to convert the apparent range frequency records into electron density profiles is contained in papers presented in *Proc. IEEE* (June, 1959).

For the present analysis, a large number of vertical profiles of electron density were provided by the NASA Ames Research Center. These profiles represented data acquired principally at Ottawa and Resolute Bay, Canada; Winkfield, England; and Stanford, California. In order to distinguish the effects of H^+ flow from other processes occurring in the top side ionosphere it is necessary to examine the electron density profile up to an altitude of at least 2000 km and preferably 2500 km. For the present analysis only those passes having electron density profiles extending above 2000 km have been used to determine local time, seasonal, and latitudinal variations in the electron density profiles.

To demonstrate the character of the reduced data, Fig. 3 presents the night-time latitudinal variation in electron density at fixed altitudes between 500 and 2500 k in steps of 500 k for 7 July 1968. The local time of this pass extends from 2317 LT at $\Lambda = 83^\circ$ to 2329 LT at $\Lambda = 38^\circ$ (all latitudes presented are geomagnetic invariant derived from the expression $\cos^2 \Lambda = 1/L$ where L is the McIlwain L parameter). The electron density contours of this figure show that the variation of electron density with altitude, measured in terms of the electron density scale height H_e defined as

$$\frac{1}{n_e} \frac{dn_e}{dz} = -\frac{1}{H_e} \quad (1)$$

depends strongly upon invariant latitude. Below the apparent density minimum near $62^\circ \Lambda$, the scale heights are relatively large (~ 1300 km) while poleward of this boundary the scale heights are smaller (~ 550 km).

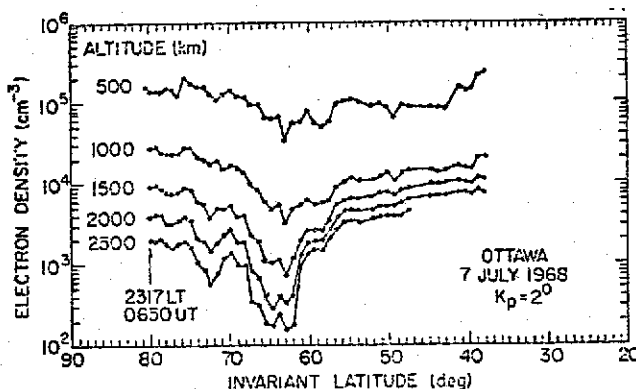


FIG. 3. CONTOURS OF TOPSIDE ELECTRON DENSITY MEASURED BY ALOUETTE-II. The plasmapause is readily apparent in the high altitude densities near $61^\circ \Lambda$ while auroral oval heating is present between 66° and $72^\circ \Lambda$.

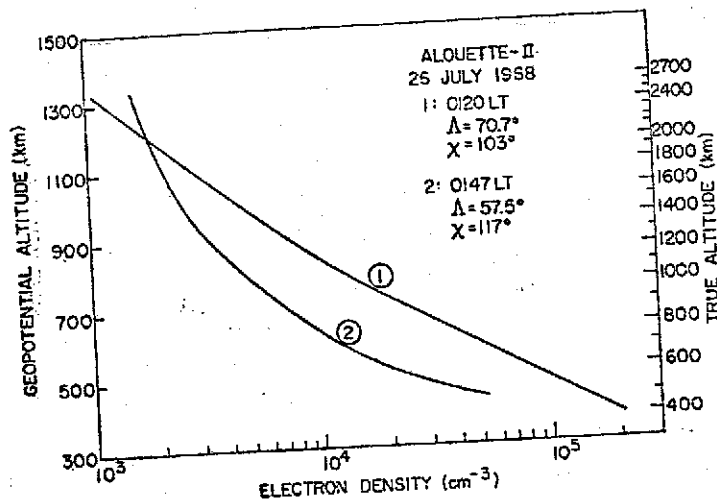


FIG. 4. ALTITUDE PROFILES OF ELECTRON DENSITY OBTAINED OUTSIDE THE PLASMASPHERE (CURVE 1) AND INSIDE THE PLASMASPHERE (CURVE 2).

Light ions are absent outside the plasmapause but, owing to the higher plasma temperature, the plasma density is actually larger than inside the plasmasphere up to an altitude of 2200 km.

The transition from large to small scale heights at $62^\circ\Lambda$, along with the simultaneous sharp decrease of electron density visible above 1500 km, represents the topside version of the plasmapause. To show the differences between the low and high latitude regions in more detail, vertical profiles of electron density obtained at $\Lambda = 70.7^\circ$ and 57.5° on 26 July 1968 are given in Fig. 4 where the densities are plotted in terms of geopotential altitudes to eliminate the variation of gravity with altitude. Using the definition of the scale height given by (1), curve 1 of Fig. 4, taken outside the plasmasphere, has a scale height of 800 km and is representative of O^+ at a plasma temperature $T_e + T_i = 8400^\circ K$. Curve 2, in contrast, has a scale height of 3000 km (at 2700 km altitude) which arises from a mixture of H^+ and O^+ .

Although it is not of direct concern to this study, the existence of a high altitude electron trough is apparent for $62^\circ \leq \Lambda \leq 67^\circ$ on 7 July 1968. The lower latitude edge corresponds to the plasmapause while the poleward boundary results from changes in scale height associated with the spatially varying enhanced temperatures in the auroral oval. Poleward of $74^\circ\Lambda$ the solar zenith angle becomes less than 100° so both photoionization and plasma heating affect the densities there.

Although data such as these provide important information regarding the dynamic character of the topside ionosphere outside the plasmapause, examination of other local time sectors has revealed the presence of equally important plasma flows inside the plasmasphere which have not been previously reported. Of particular importance are upward flows of thermal H^+ found in the summer plasmasphere in the 07–14 hr LT sector. To illustrate this feature, several latitudinal electron density profiles obtained in June and July 1966 at Stanford and Winkfield are shown in Figs. 5–7 for local times between 0700 and 0800 when the solar zenith angle was less than 55° . For all three passes the maximum K_p at the start of the pass was less than 1. For the data of 3 July, 1966 the maximum K_p in the preceding 7 days was 2^+ .

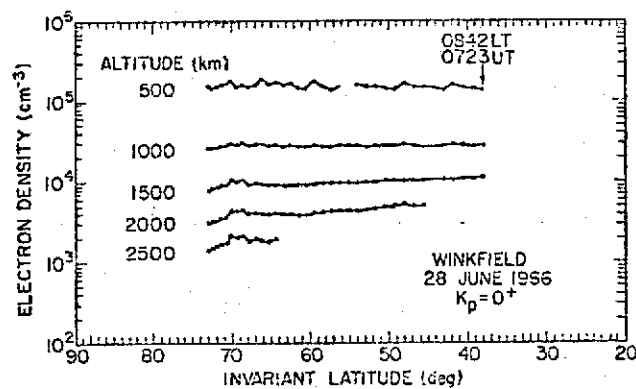


FIG. 5. SUMMER MORNING CONTOURS OF ELECTRON DENSITY FOR 28 JUNE 1966. THERE IS NO INDICATION OF LIGHT IONS.

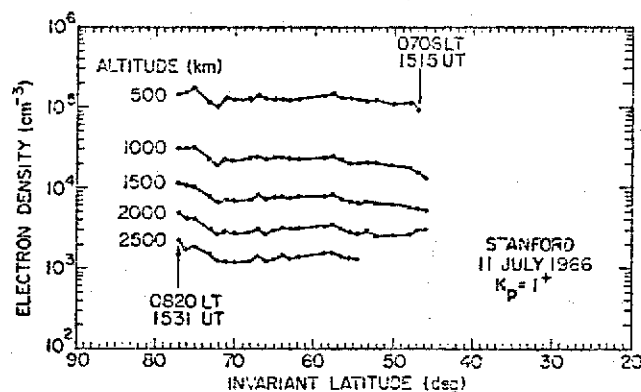


FIG. 6. SUMMER MORNING CONTOURS OF ELECTRON DENSITY FOR 11 JULY 1966.

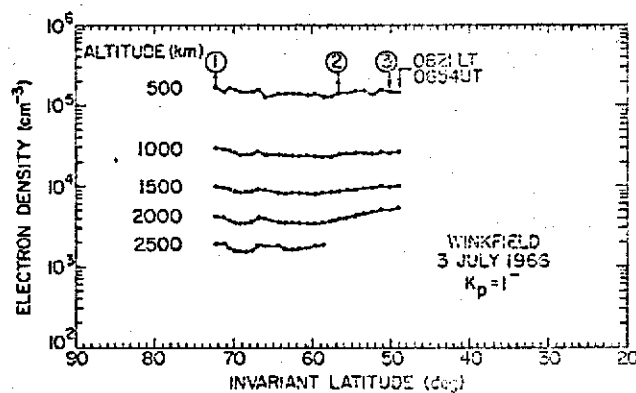


FIG. 7. SUMMER MORNING CONTOURS OF ELECTRON DENSITY FOR 3 JULY 1966.

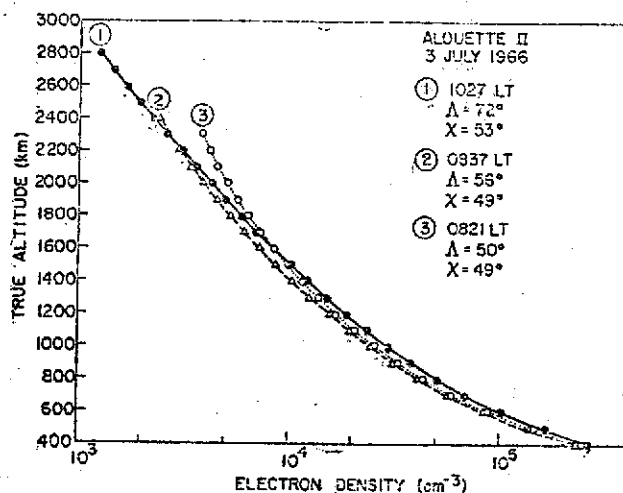


FIG. 8. VERTICAL PROFILES OF ELECTRON DENSITY FOR 3 JULY 1966 AT THREE POINTS INDICATED ON FIG. 7.

These profiles show that O^+ is the dominant to at least 2500 km and, as discussed in the text, an upward flow of about $3 \times 10^8 H^+$ ions $cm^{-2} sec^{-1}$ must be present.

In contrast to the night-time latitudinal profile given in Fig. 3, no discontinuity in plasma density or scale height is evident at any of the observed invariant latitudes. The scale heights are small (300–600 km) and characteristic of O^+ alone. There is little day to day variability present at high altitudes (1500–2500 km) which does not arise from changes in the F_2 -layer densities; i.e. normalization with respect to the 500 km densities tends to produce topside densities which are virtually unchanged from day to day. Thus, it is possible to accept the data of those figures as typical for summer morning conditions.

Typical profiles of electron density as a function of altitude, taken from the pass of July 3 1966, (see Fig. 7) are shown in Fig. 8 for $\Lambda = 72^\circ$, 56° and 50° . When the effect of gravitational variation is removed, it is found that there is no important change in scale height up to 2400 km altitude other than that due to a small increase in plasma temperature. As discussed in the next section, such a behavior for the observed conditions can be explained only through the presence of an upwards H^+ flow of magnitude 10^8 ions $cm^{-2} sec^{-1}$.

To show that such a behavior is not directly related to magnetic activity, Fig. 9 shows the latitudinal contours obtained on 9 July 1966 when successive disturbances culminated in a K_p of 6 at the time of the pass. In spite of this activity, the results of Fig. 9 are similar to the data of Figs. 5–7 and there is no high altitude plasmopause present to $\Lambda = 45^\circ$ even though a jump occurs in the 500 km base density. Note, however, that the plasma scale heights are the same on both sides of this change. Such a lack of a topside plasma density discontinuity provides a distinct contrast to satellite measurements made further away from the Earth nearer the equatorial plane where a plasmopause is normally present. (Taylor *et al.*, 1965, 1968; Chappell *et al.*, 1970, 1971).

In order to relate the Alouette-II electron density profiles to the physical processes associated with the distribution of ions and electrons in the topside ionosphere, it is necessary to introduce the equations describing the behavior of multi-ion plasmas. In the following analysis procedure, models of the topside ionosphere are constructed to match the observed profiles. The essential problem is to explain why light ions (H^+ or He^+) are

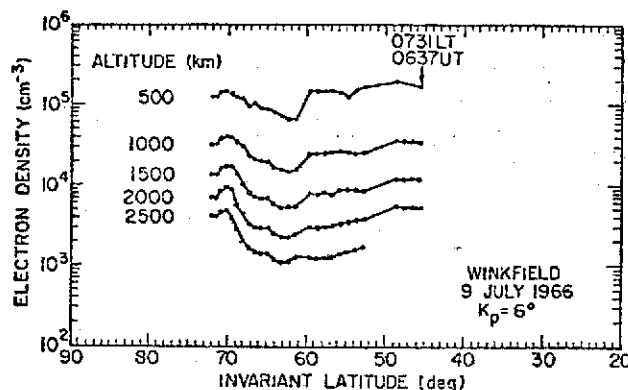


FIG. 9. SUMMER MORNING CONTOURS OF ELECTRON DENSITY DURING DISTURBED MAGNETIC CONDITIONS.

Auroral oval heating is present near 70° A while variations in the 500 km density are reflected in variations at higher altitudes.

absent from the summer morning topside ionosphere; i.e. why the typical heavy to light ion transition so readily apparent in the night-time data (compare curves 1 and 2 of Fig. 4) is absent in the morning sector (curves 1-3 of Fig. 8). Using the models developed in the next section it is found that such a behavior can only be explained if there is an upward flow of H^+ and He^+ .

3. FLOW EQUATIONS FOR THE TOPSIDE IONOSPHERE

To analyze the electron density profiles described in the last section we must establish a model for the topside ionosphere. Relying upon previous experimental results (Taylor *et al.*, 1965, 1968; Hoffman, 1969 and others) and theory we assume that O^+ is the dominant ion in the F_2 -region and that H^+ is present at higher altitudes. (While there is a possibility that He^+ may be present, it cannot affect the present analysis since the models must explain the absence of all light ions.)

For the present model we assume that O^+ is the dominant ion at 400 km. Owing to diurnal changes in ionization rates, neutral wind momentum transfer, and electrodynamic drifts, short and long term variations are normally present in the O^+ density. Thermal H^+ is present in these same regions as a consequence of the accidentally resonant reaction.



with $k_f = 2.5 \times 10^{-11} T_n^{1/2} n(H) \text{ sec}^{-1}$ and $k_b = 2.2 \times 10^{-11} T_i^{1/2} n(O) \text{ sec}^{-1}$ (Banks and Kockarts, 1973).

In chemical equilibrium the ratio $n(H^+)/n(O^+)$ can be obtained as

$$\frac{n(H^+)}{n(O^+)} = \frac{9}{8} \frac{n(H)}{n(O)} \left(\frac{T_n}{T_i} \right)^{1/2} \quad (3)$$

so that at 500 km H^+ is a minor constituent when thermospheric temperatures are greater than 800°K. The time constant associated with the equilibrium condition given by (3) is short, ranging from 220 sec in a 750°K thermosphere to 1.7 sec at 2000°K (Banks and Kockarts, 1973).

Above 700-800 km the condition of chemical equilibrium between O^+ and H^+ becomes increasingly difficult to maintain owing to the effects of ion transport arising from plasma pressure gradients and gravity. To describe the electron density profiles discussed in the

last section, steady state solutions to the equations for the density and flow speed of a plasma composed of O^+ and H^+ are needed. Generally speaking, such a procedure involves the coupled equations of continuity and momentum conservation for both O^+ and H^+ (see Banks and Holzer, 1969b). However, since the O^+ flux is much smaller than the O^+-O limiting flux ($\sim 2 \times 10^9$ ions $cm^{-2} sec^{-1}$), it is possible to ignore the effect the O^+ flow velocity has upon the O^+ density profile (Banks and Holzer, 1969b; Schunk and Walker, 1970). In this situation the equation of O^+ momentum conservation can be written as

$$\frac{1}{n(O^+)} \frac{dp(O^+)}{ds} + \frac{1}{n_e} \frac{dp_e}{ds} + m(O^+)g_{\parallel} = m(O^+)\nu(O^+, H^+)v(H^+) \quad (4)$$

where s is a coordinate along the magnetic field, $p(O^+) = n(O^+)kT_i$, $p_e = n_e kT_e$, $n_e = n(O^+) + n(H^+)$, g_{\parallel} is the component of gravity parallel to the magnetic field, $\nu(O^+, H^+)$ is the O^+-H^+ diffusion collision frequency, and $v(H^+)$ is the H^+ speed along the magnetic field.

With regard to H^+ , flow effects cannot be ignored and the density and flow velocity must be found from the equations

$$\frac{d}{ds} [n(H^+)v(H^+)] = q(H^+) - \beta(H^+)n(H^+) \quad (5)$$

$$\frac{1}{n(H^+)} \frac{dp(H^+)}{ds} + \frac{1}{n_e} \frac{dp_e}{ds} + m(H^+)g = -m(H^+)\nu(H^+, O^+)v(H^+) \quad (6)$$

where $q(H^+) = n(O^+)n(H^+)k_f$, $\beta(H^+) = n(O^+)k_b$, $p(H^+) = n(H^+)kT_i$, and other quantities are similar to those given in Equation (4).

To obtain the theoretical profiles of ion composition it is necessary to solve Equations (4)–(6) subject to given boundary values. If $v(H^+) = 0$, such solutions describe diffusive equilibrium while if $v(H^+) \neq 0$, the general flow solutions are obtained describing inward and outward motions (Geisler and Bowhill, 1965; Geisler, 1967; Banks and Holzer, 1969b; Banks *et al.*, 1971; Schunk and Walker, 1970).

For the present study it is necessary to compute ion density profiles consistent with the observed electron density and the inferred values of atmospheric parameters. This was done in the following way to obtain profiles over the altitude range 500–3000 km: the observed electron density at 500 km was taken to be a result of H^+ and O^+ in chemical equilibrium using Equation (3). Values of the neutral atomic hydrogen density were taken from the satellite results of Mayr and Brinton (1971) for June and July 1966. The density of atomic oxygen was inferred from CIRA (1955) models based on the solar 10.7 cm radio flux with correction for magnetic activity.

In addition to this information, the solution to the coupled ion equations requires an additional condition relating to the density or flux of H^+ at the upper boundary. As shown later, the H^+ flux is a relatively poor boundary condition and for this study solutions to the H^+ flow equations were obtained by choosing a specific value of the H^+ density at 3000 km. Through variation of this upper boundary density it was possible to match the observed electron density profile with sufficient accuracy to determine the magnitude of the flux flowing along the magnetic field lines.

To illustrate this method, Fig. 10 shows the family of H^+ density profiles appropriate to a 1000°K thermosphere taken from the models of Banks and Kockarts (1973). The

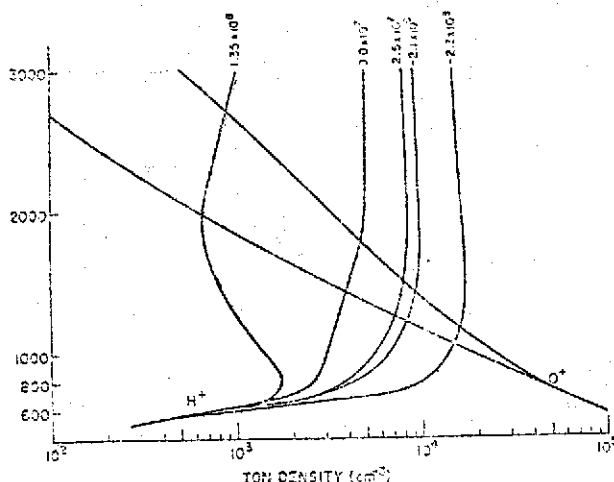


FIG. 10. COMPUTED H^+ AND O^+ DENSITY PROFILES FOR DIFFERENT H^+ FLUXES AT 3000 km. The O^+ density is largest for the smallest H^+ profile, and *vice versa*. A 1000°K thermosphere was used with a 500 km neutral hydrogen density of $1.92 \times 10^5 \text{ cm}^{-3}$. The plasma temperature ($T_e + T_i$) at 3000 km was taken as 6500°K.

electron temperature profile was computed using an electron heat flux of $5 \times 10^9 \text{ eV cm}^{-2} \text{ sec}^{-1}$ with a boundary value $T_e(500 \text{ km}) = 2500^\circ\text{K}$ and the usual electron gas thermal conductivity. The ion temperature profile was obtained using the ion energy balance equations described by Banks (1967) without thermal conduction. For this example the magnetic field was assumed to be vertical.

The individual H^+ profiles given by Fig. 10 correspond to different H^+ densities at 3000 km ($10^3, 5 \times 10^3, 8 \times 10^3, 9 \times 10^3, 1.5 \times 10^4 \text{ ions cm}^{-3}$). Associated with each of these profiles is a computed H^+ flux, the magnitude being given directly above each curve. Positive values of the flux correspond to outward flows, negative values show inward flows.

The range of O^+ density for the different H^+ profiles is indicated by the shaded region of Fig. 10. When H^+ is the dominant ion, the O^+ density falls off most rapidly with altitude, while when O^+ is dominant, the slowest decrease is appropriate. This behavior results from the electric field coupling between O^+ and H^+ and provides an explanation for the rapid ion composition changes observed near the plasmapause where H^+ flow becomes important (see Banks (1970) for a more detailed discussion of this effect).

For the purposes of the present study, the most important characteristic of the density profiles given in Fig. 10 is the abrupt change in scale height associated with the transition of the major ion species from O^+ to H^+ . For the summer daytime data discussed here, no such transition was observable in the electron density profiles up to altitudes of 2000–2500 km. Consequently, it is necessary to suppose that the H^+ density is low at the upper boundary and, as a consequence, that an outward H^+ flow is present.

Although it might be thought that the matching of theory and experiment using this method would give only crude estimates of the H^+ flux, this is not necessarily the case owing to a saturation effect which limits the magnitude of the flux for a wide range of H^+ boundary densities. To show this effect, the value of the H^+ flux has been plotted in Fig. 11 as a function of the 3000 km H^+ density using the results of Fig. 10. From this plot we find that diffusion equilibrium (i.e. no H^+ flux) occurs when $n(H^+)_{3000} \approx 9 \times 10^3 \text{ cm}^{-3}$. For H^+ densities greater than this value, the flux is inward with a magnitude which increases

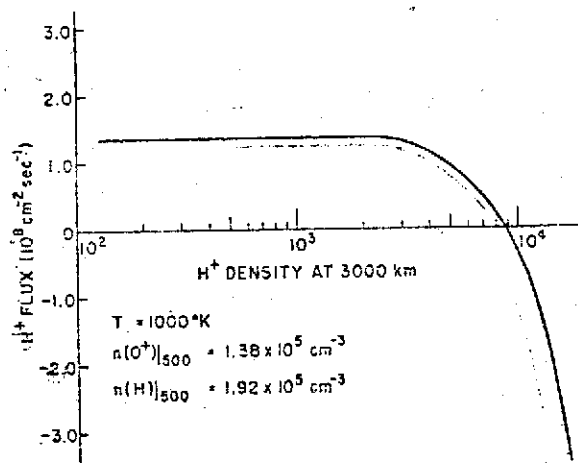


FIG. 11. VARIATION OF THE H^+ FLUX AS A FUNCTION OF THE 3000 km H^+ DENSITY.

The effect of flux saturation occurs quickly and limits the rate at which H^+ can leave the topside ionosphere. In contrast, there is no limit to the rate at which H^+ can flow into the ionosphere.

rapidly with increasing H^+ density. Such a result indicates that any excess plasma contained in field tubes above 3000 km can be readily transferred downwards to the upper F-region.

When the H^+ boundary density is lowered below the diffusive equilibrium value an outward H^+ flux is established. Unlike the inward flow, however, the outward flow rapidly saturates such that the H^+ flux soon reaches a limiting value and further decreases in the H^+ boundary density yield no corresponding change in flux. This behavior illustrates one aspect of the limiting flux concept discussed by Hanson and Patterson (1964) and Geisler (1967).

To apply the limiting flux idea to the present study the following line of reasoning has been used: the H^+ flux in saturation region depends only slightly upon H^+ density when the H^+ density is less than the diffusive equilibrium value. Thus, if we assume that the H^+ boundary density is equal to the measured electron density at the satellite, we can compute a lower limit to the flux. Actually, since there is no change in electron density scale height seen at this upper altitude for the present data, the true H^+ density must be much less than the electron density. However, owing to the H^+ flux saturation effect, the use of the true, lower H^+ density in the computation would not appreciably change the computed value of the flux.

While the above reasoning permits us to compute the H^+ flux when the electron density profile indicates the absence of appreciable amounts of H^+ , difficulties arise when the H^+ and O^+ densities become comparable near 2500 km. Reference to Figs. 10 and 11 shows that the H^+ flow is very sensitive to small changes in the upper boundary density of H^+ when H^+ is the dominant ion above about 1500 km. In this situation small changes in the H^+ density can lead to large changes in the flux and, consequently, the measured electron density profiles cannot be used to predict accurately either the sign or the magnitude of the flux. Thus, for example, it is not possible to use the profiles shown in Fig. 3 to compute H^+ fluxes in the regions inside the plasmasphere. Although the apparent change in scale height shows the presence of H^+ (or perhaps He^+), the uncertainties in temperature, ion

composition, and atmospheric densities are sufficient to make any computation highly inaccurate.

Although chemical and flow effects are most important in determining the overall ion composition profiles, the thermal structure associated with the electron and ion temperatures cannot be neglected. Reference to Equations (4) and (6) clearly indicates that values of the temperatures and their gradients play a part in determining the final result. For the present data direct measurements of temperature were not available from the Alouette-II spacecraft. However, the companion satellite, Explorer 31, did carry an electron temperature probe which provided (Brace, personal communication) typical latitudinal profiles of electron temperature for the periods considered here.

Solutions for the present model require that the electron and ion temperatures be specified as functions of altitude. Because the electron density scale heights were uniformly small (<600 km) for the summer morning passes used here, it was possible to assume that O^+ was close to a diffusive equilibrium distribution. Using the experimentally observed density distributions it was then possible to solve the equation

$$\frac{1}{T_p} \frac{dT_p}{ds} + \frac{m(O^+)g_{\parallel}}{kT_p} + \frac{1}{n_e} \frac{dn_e}{ds} = 0 \quad (7)$$

for the plasma temperature, $T_p = T_e + T_i$, by integrating downward from the satellite. The initial value of T_p at the satellite was estimated directly from the slope of the electron density scale height at the satellite assuming that O^+ was the dominant ion. Using this value, Equation (7) could then be used to obtain the plasma temperature, T_p , as a function of altitude.

It is difficult to estimate the errors in the analysis for the temperature profile. The values of T_p deduced for the satellite altitude, however, agreed closely with the Explorer-31 measurements. In addition, changes in composition from O^+ to H^+ or He^+ would give an apparent T_p higher than true value. Using this method, profiles for T_p were deduced showing thermal gradients of 0.5 – $1.0^\circ K km^{-1}$. Such gradients slightly modify the H^+ density profile by making the scale height of H^+ smaller than would be found for isothermal conditions. However, it does not obscure the transition from O^+ to H^+ nor change in any important way the H^+ limiting flux.

After the value of T_p was determined, computations of T_e and T_i were made by assuming steady state conditions for the exchange of thermal energy between electrons, ions, and neutrals using rates previously given (see, for example, Banks and Kockarts, 1973).

4. RESULTS

Using the mathematical models of the last section, calculations have been made of the H^+ flow associated with the typical summer morning Alouette-II pass shown in Fig. 7. For this calculation, the neutral hydrogen density was taken from the results of Mayr and Brinton (1971). The densities of other constituents were determined from standard CIRA (1965) atmospheric models.

During this summer period the electron density profiles associated with the Alouette-II data give no indication of H^+ . Thus, to determine the H^+ flux, the computed ion composition profiles have been made assuming that H^+ density at the satellite altitude is equal to the observed electron density. As mentioned before, if H^+ were really the dominant ion near the satellite, then the electron density scale height would be many times larger than the values which were observed; the adopted procedure gives an upper limit to the

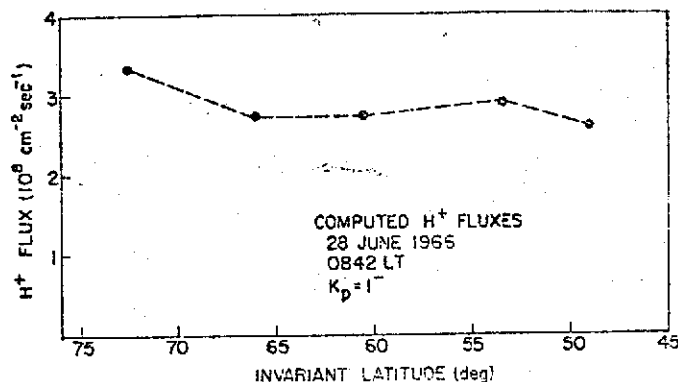


FIG. 12. COMPUTED H^+ FLUXES FOR 28 JUNE 1966, SPANNING THE RANGE OF THE NORMAL MORNING PLASMAPAUSE.

These results show that a large upward surge of H^+ must enter the plasmasphere in the morning sector.

amount of H^+ actually present and a lower limit to the upward H^+ flux. Using this method the H^+ vertical flux has been obtained as a function of latitude for the data of Fig. 7 and is plotted in Fig. 12. The slight variation of vertical flux with latitude results principally from the progressively greater dip angle of the magnetic field. Comparison of Figs. 6 and 13 shows that changes in the electron density profile with latitude introduce very little variation in the flux, and there is no flux discontinuity between the polar wind regions assumed to exist above $60^\circ A$ and the interior of the morning plasmasphere extending down to $L = 2.3$.

The results given by Fig. 12 are typical of all morning sector data examined for the summers of 1966, 1967 and 1968. However, owing to a lack of atomic hydrogen density data no attempt has been made to compute H^+ fluxes for the later periods. As shown elsewhere (Gaisler, 1967; Banks and Holzer, 1969b), the limiting H^+ flux is directly proportional to the atomic hydrogen concentration near 600–800 km. On this basis it might be expected that these later fluxes would be substantially smaller than those found for 1966. A further difficulty, however, lies in the fact that by decreasing the atomic hydrogen concentration one moves the normal, non-flow O^+/H^+ transition point to higher altitudes. Thus, to measure accurately the effects of flow when the hydrogen densities are low, one must have data extending to altitudes higher than the Alouette-II orbit.

Examination of the local time behavior of the deduced plasma flow is made difficult by the orbital relationships between altitude, local time and season. However, analysis of electron density for the summer periods in 1967–1970 indicates that the upward flow seems to be present through about 13–14 hr LT. In 1968, however, the neutral hydrogen densities were much lower than in 1966 and the deduction of H^+ flow could be made only during passes where the electron density profile was obtained up to at least 2500 km altitude.

5. DISCUSSION

The H^+ fluxes described here appear to be a normal feature of the morning sector of the plasmasphere. Although magnetic storms are thought to give similar flows, the data used in this study show no obvious differences between observations made after many magnetically undisturbed days and those obtained during such periods (compare the contours of Figs. 5–7 with Figs. 9).

The strength of the flow is sufficiently large to deplete greatly H^+ in the topside ionosphere and greatly alter the O^+/H^+ transition altitude. In this situation it is not possible to distinguish the plasmapause at these altitudes, i.e. there is no essential difference between the high latitude polar wind and the present flow observed at midlatitudes. Such a conclusion may also be supported by a recent study of topside troughs by Tulunay and Sayers (1971) where there were essentially no density troughs observed in the morning sector at Ariel altitudes. However, the Ariel data also reflect changes in composition arising from thermal effects. At higher altitudes of Alouette-II, however, the reason for such an absence of light ions clearly relates to the lack of H^+ or He^+ inside the plasmasphere at ionospheric heights; i.e. a flow of light ions is present. Even though the plasmapause is not apparent in the topside ionosphere there appears to be no ambiguity in satellite measurements made further away from the Earth where the H^+ density is observed to drop to low densities without any indication of a decrease in plasmapause latitude (Chappell, personal communication). This lack of correspondence has not yet been adequately explained.

Incoherent scatter measurements of plasma density and drift velocity can also provide information about the H^+ fluxes described here. At Millstone Hill ($L = 3.1$), Evans (1971a,b) has observed large upwards O^+ fluxes following sunrise and continuing through late morning hours. Although a large fraction of this flow is associated with the thermal expansion of the O^+ in the topside ionosphere resulting from increases in plasma temperature, there appears to be a residual component associated with O^+-H charge exchange and subsequent H^+ flow. Using Millstone Hill data for 23-24 March 1970 Nagy and Banks (1972) made computations of the diurnal H^+ flux and density arising from changes in O^+ density at 500 km. The results indicate an upward flux throughout most of the morning. However, the H^+ density at 3000 km was computed to be about $2 \times 10^4 \text{ cm}^{-3}$, about a factor of ten larger than is observed in the same local time sector by Alouette-II.

Although the existence of the morning H^+ flow appears definite, the causative mechanism remains to be identified. The flow itself represents the effect of plasma pressure gradients along the magnetic field. It is possible that the flow arises as a replenishment of ionization previously lost to the F_2 -layer via H^+-O charge exchange during the summer night. As shown by Fig. 1, the plasmasphere undoubtedly acts as a reservoir of ions which are able to flow into the F_2 -region when the O^+ pressure is sufficiently low (Hanson and Patterson, 1964). Following sunrise, the F_2 -region O^+ densities rise rapidly due to photoionization and, owing to O^+-H charge exchange there is a consequent H^+ flow upwards into plasmasphere.

Although the reservoir idea may be partially correct, it ignores the effects of transverse electric fields associated with the penetration of the magnetospheric electric field into the plasmasphere. Such electric fields on the morningside of the plasmasphere have a tendency to drive plasma away from the Earth (see Sharp *et al.*, 1972) so that a pressure gradient is established along the magnetic field driving plasma (H^+) upwards. Such an effect should be readily seen in the F_2 -region as a poleward drift of the F -region plasma. This plasma is not lost from the Earth, however, since the opposite effect takes place in the evening sector of the plasmasphere where plasma is driven inwards (compressed) and downward flows of plasma must remove excess ionization from the field tube reservoirs.

Finally, it is possible that the flow represents a transfer of ions between summer and winter conjugate regions (Mayr *et al.*, 1972). Such a flow could arise from the presence of differential pressures between the conjugate F -regions. In addition, the influx of ionization

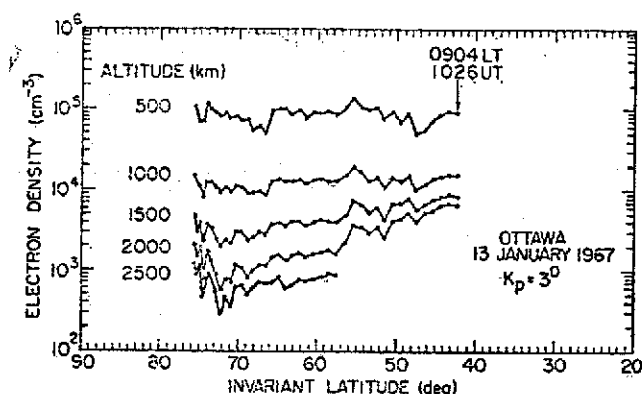


FIG. 13. ELECTRON DENSITY CONTOURS FOR WINTER MORNING CONDITIONS.

There is no evidence for large H^+ flows from the conjugate region although light ions are present below $58^\circ A$.

can result in substantially greater H^+ densities in the winter topside ionosphere. In connection with this possibility, a typical winter morning pass of Alouette-II as seen at Ottawa is shown in Fig. 13. Although the crowding of electron density contours at low latitudes is suggestive of an H^+ influx, a strong solar zenith angle dependence is also present leading to considerable variation in plasma temperature and F_2 -region densities. Examination of records of this type has not provided any definite support for the idea of plasma flow between conjugate hemispheres.

From the foregoing discussion, it appears that while the presence of a large scale H^+ flow in the morning sector of the plasmasphere seems well established, its cause remains to be determined.

Acknowledgements—We wish to acknowledge many useful discussions with Dr. C. R. Chappell. The Alouette-II data were provided by Drs. L. Coffin and K. L. Chan, while Dr. L. Brace provided unpublished electron temperature data from Explorer 31. This research was supported in part by NSF grant GA 30351 and NASA grant NGR 05-002-075 at the University of California, San Diego and by NSF grants GA-23042 and GA-32590X at Stanford University.

REFERENCES

- BANKS, P. M. (1967). *J. geophys. Res.* **72**, 3365.
 BANKS, P. M. (1972). In *Magnetosphere-Ionosphere Interactions* (Ed. K. Foldestad) p. 87. University of Oslo Press.
 BANKS, P. M. and HOLZER, T. E. (1969a). *J. geophys. Res.* **74**, 6317.
 BANKS, P. M. and HOLZER, T. E. (1969b). *J. geophys. Res.* **74**, 6304.
 BANKS, P. M. and KOCKARTS, G. (1973). *Aeronomy*. Academic Press, New York.
 BANKS, P. M. and NAGY, A. F. (1972). *J. geophys. Res.* **77**, 4277.
 BAUER, S. J. (1966). *Annls geophys.* **22**, 247.
 BRINTON, H. C., GREBOWSKY, J. M. and MAYR, H. G. (1971). *J. geophys. Res.* **76**, 3738.
 CHAPPELL, C. R. (1972). *Rev. Geophys.* **10**, 951.
 CHAPPELL, C. R., HARRIS, K. K. and SHARP, G. W. (1970). *J. geophys. Res.* **75**, 50.
 CHAPPELL, C. R., HARRIS, K. K. and SHARP, G. W. (1971). *J. geophys. Res.* **75**, 7632.
 EVANS, J. V. (1971a). *Radio Sci.* **6**, 609.
 EVANS, J. V. (1971b). *Radio Sci.* **6**, 843.
 GEISLER, J. E. and BOWHILL, S. A. (1965). *J. atoms. terr. Phys.* **27**, 119.
 HANEON, W. B. and PATTERSON, T. N. L. (1964). *Planet. Space Sci.* **12**, 979.
 HO, M. C. and MOORCROFT, D. R. (1971). *Planet. Space Sci.* **19**, 1441.
 HOFFMAN, J. H. (1969). *Proc. IEEE* **57**, 1063.
 KOCKARTS, G. and NICOLET, M. (1963). *Annls geophys.* **19**, 370.
 MANGE, P. (1960). *J. geophys. Res.* **65**, 3833.

- MARUBASHI, K. (1970). *Rep. Atmosph. Space Res. Japan* 24, 322.
- MAYR, H. G. and BRINTON, H. C. (1971). *J. geophys. Res.* 76, 3738.
- MAYR, H. C., FONTHEIM, E. G., ERACE, L. H., BRINTON, H. C. and TAYLOR, H. A. (1972). *J. atoms. terr. Phys.* 34, 1659.
- MAYR, H. G., GREBOWSKY, J. M. and TAYLOR, H. A. (1970). *Planet. Space Sci.* 18, 1123.
- MOFFETT, R. J. and MURPHY, J. A. (1973). *Planet. Space Sci.* 21, 43.
- PARK, C. G. (1970). *J. geophys. Res.* 75, 4249.
- RUSH, C. M. and VENKATESWARAN, S. V. (1965). *Rev. Geophys.* 3, 463.
- SCHUNK, R. W. and WALKER, J. C. G. (1970). *Planet. Space Sci.* 18, 1319.
- SCHUNK, R. W. and WALKER, J. C. G. (1972). *Planet. Space Sci.* 20, 581.
- SHARP, G. W., CHAPPELL, C. R. and HARRIS, K. K. (1972). In *Magnetosphere-Ionosphere Interactions* (Ed. K. Foldestad). p.169, University of Oslo Press.
- TAYLOR, H. A., BRINTON, H. C. and PHARO, M. W. (1968). *J. geophys. Res.* 73, 961.
- TAYLOR, H. A., BRINTON, H. C., PHARO, M. W. and RAHMAN, N. K. (1968). *J. geophys. Res.* 73, 5521.
- TAYLOR, H. A., BRINTON, H. C. and SMITH, C. R. (1965). *J. geophys. Res.* 70, 5769.
- TULUNAY, Y. and SAYERS, J. (1971). *J. atoms. terr. Phys.* 33, 1737.

ATTACHMENT III

The Physical Connection Between the Plasmasphere and
the Midlatitude Ionospheric Trough

C. R. Chappell^{*} and P. M. Banks
Department of Applied Physics and Information Science
University of California at San Diego
La Jolla, California 92037

Submitted to Journal of Geophysical Research

November, 1973

* Permanent address: Lockheed Palo Alto Research Laboratory
3251 Hanover Street
Palo Alto, California 94304

Abstract

Previous statistical studies on the connection between the midlatitude ion/electron trough and the plasmapause have employed a variety of primarily non-physical definitions for the trough position and, consequently, have left the association of the two regions unclear. In this paper we examine these studies and propose a physically motivated definition of the midlatitude trough position which, in combination with new information of the filling state of the plasmasphere, leads to a clear picture of the connection between the midlatitude trough and the plasmasphere. We find that within the plasmasphere the important boundary which influences the midlatitude trough is the transition from the inner to the outer plasmasphere. This boundary, and the trough, coincide with the plasmapause only under special conditions. The inclusion of the inner-outer plasmasphere boundary in the general picture of the thermal plasma distribution in the inner magnetosphere leads to an understanding of the relationship between the midlatitude ion/electron trough, the plasmasphere and the plasmapause.

The Physical Connection Between the Plasmasphere and the Midlatitude Ionospheric Trough

C. R. Chappell and P. M. Banks
Department of Applied Physics and Information Science
University of California, San Diego
La Jolla, California 92037

Introduction

There has been a great deal of work done to relate the midlatitude trough that appears in electron and ion density in the ionospheric F-layer to the plasmopause which is observed at higher altitudes in the magnetosphere, [Carpenter, 1965, Chappell, 1972]. Since the first observations of the midlatitude trough by Muldrew (1965) from Alouette I sounder data and by Sharp (1966) from in situ ion measurements, various authors have sought to connect the magnetospheric and ionospheric results with a simple physical explanation [Thomas and Andrews, 1968; Rycroft and Thomas, 1970; Rycroft and Burnell, 1970; Mayr, et al., 1970]. In these studies limited success has been achieved, at least for the nightside region, between local times of 2100 LT and 0600 LT. But if the underlying assumptions and definitions of these studies are examined closely, one finds that the commonality of the ion trough and the plasmopause is far from established. And, in fact, one finds that physical processes other than those discussed by previous authors may play the dominant role in establishing the midlatitude ion trough at a position different from the ionospheric projection of the equatorial plasmopause.

In this paper we first examine the results of the early statistical studies of the location of the trough and plasmopause. Following this, we present new data on plasmasphere and ion trough characteristics which offer a potential key to understanding their association. Finally, we present computed models of the

topside ionosphere for diffusive equilibrium and ion flow situations to show how these models can qualitatively explain the ionosphere and plasmasphere observations and provide a link between these two geophysical phenomena.

Previous Studies of the Midlatitude Trough - Plasmopause Association

The early studies of the coincidence of the trough and plasmopause locations were based on electron and ion density measurements made in the topside ionosphere by radio sounders and in situ probes on polar orbiting satellites as compared with plasmopause measurements made by the whistler technique [Thomas and Andrews, 1968; Rycroft and Thomas, 1970; Rycroft and Burnell, 1970; Muldrew, 1971; Brace and Theis, 1973]. The regions of the inner magnetosphere involved in these comparisons are illustrated in Figure 1. Here we show the inner magnetosphere with the ionosphere and plasmasphere as prominent features. The specific regions under comparison are illustrated by partial satellite orbital tracks with comparison sketches of the expected electron or total ion density profiles. (The difference between the electron and light ion density profiles is discussed later in this paper.) The dashed curve represents the track of a polar orbiting satellite in the topside ionosphere which measures the midlatitude trough region as illustrated in the upper sketch. The dotted track covers the equatorial plasmopause region with the density profile illustrated in the lower sketch. This lower sketch can be derived both from whistler observations and direct satellite measurements. Given the existence of the two pertinent sets of data it is natural to compare the results and ask in what way do the trough and plasmopause compare in position and if they differ, why do they, physically?

Figure 2 shows a specific example of in situ ion composition data measured in the topside ionosphere by the ion mass spectrometer on Ogo 4 (Taylor, Private Communication). Note the trough locations formed by the decreasing H^+ and the increasing O^+ (not too pronounced in this case) in the

region of about 40° to 70° dipole latitude on either side of the magnetic equator. A trough appears very prominently in the H^+ ion density as a decrease of about three orders of magnitude through 40° to 70° dipole latitude. A transition from H^+ dominance to O^+ dominance is also seen at the trough. This is a typical effect at the nightside trough location associated with outward flow of H^+ and has been discussed by Binton et al., 1971 (also, in theoretical detail, in Banks, 1972).

The low latitude side of the nightside trough is generally attributed to the presence of the plasmasphere while the high latitude side or "cliff" [Rycroft and Thomas, 1970] is attributed to enhanced ionization and higher plasma temperatures resulting from auroral precipitation.

It is important in Figure 2 to note the very broad range of dipole latitudes over which the H^+ density decreases; i.e., on the low latitude side of the trough the initial decrease begins at 30° and extends to 60° dip latitude. In L-value this latitude range is approximately from $L=1.4$ to 4. This spread in L value is comparable to the maximum variation in position of the equatorial plasmopause during moderate to disturbed magnetic conditions and leaves open a broad range of latitude at which the trough position could be defined. It must also be noted that the spread of L-shells of the H^+ density decrease on the low latitude side of the midlatitude trough differs from that seen at the plasmopause where the decrease is generally much more pronounced (up to three orders of magnitude) and is confined to a few tenths of an L-shell which is about 2° of latitude at $L=4$. Typical examples of the sharpness of the equatorial plasmopause can be seen in the results of Carpenter, 1966; Taylor et al., 1970; and Chappell, 1972.

From the foregoing, it is clear that in making a comparative study between the ionospheric trough position and the equatorial plasmopause position, one is

forced to adopt specific definitions of each, and this is where the problems have developed.

Identification of the plasmopause position outside the ionosphere is not difficult, although there has been some discussion over whether the 100 ion/cm^3 on the 10 ion/cm^3 density level or the maximum density gradient position should be used (see Chappell et al., 1970). The density gradient at the plasmopause is generally steep enough and prominent enough in most cases that any of the above choices gives essentially the same result within an accuracy of a few tenths of an L-shell.

Such is not the case, however, with the midlatitude trough position. The wide range of L-shells covered by the trough has led to a number of ad hoc definitions. Three definitions employed in earlier trough studies are shown in Figure 3. In these examples the troughs were defined in terms of the total electron density and therefore represent the latitudinal profile which results from the summation of the separate ion densities, i.e., from Figure 2, primarily H^+ and O^+ . Rycroft and Thomas, 1970 (part (a)), chose the minimum electron density point in the midlatitude trough to define the trough location. In contrast, Miller, 1970 (part (b)), felt that the change in slope at the low latitude side of the trough bottom provided a more meaningful definition. Brace and Theis, 1973, chose an intermediate point where a straight line approximation to the electron density profile on the low latitude side of the trough crossed the $1000 \text{ electron/cm}^3$ point.

Each of these definitions gives a wide variation in the L-shell of the individually defined trough positions and, consequently, leads to questionable results when comparisons are made with the equatorial plasmopause location.

Moreover, it appears that the definitions of the trough location are consistent only with the general idea that the midlatitude trough must be

associated in some way with the density decrease at the equatorial plasma-pause. In retrospect, it appears that a more physically significant definition may have been overlooked completely. From current theories of ionospheric-magnetospheric coupling, one would expect that the physically important point in the midlatitude trough profiles is the point where the density begins to decrease on the low latitude side of the trough because it is there that changes begin to take place in the distribution of ionization in the topside ionosphere as a consequence of upward light ion flow. There are certainly variations in density at low latitudes associated with neutral winds and perpendicular electric fields which may occasionally confuse the initial density decrease point. However it is possible in most profiles to identify the point where the density begins to decrease, forming the low latitude side of the trough. In the data presented from sounder and in situ probe experiments to date this point is generally found in the range of $L=2$ to 3. Statistically, this point is approximately two L-shells inside the plasmopause position and this glaring difference may have obscured its importance. Whatever the motivating reasons, the previous trough definitions are non-physical in nature and consequently have led to some confusion in understanding the physical relationship between the trough and the plasmopause. As we show here, the use of the point of initial density decrease on the low latitude side of the trough can lead to a clear picture of the trough and plasmopause association in terms of ionospheric-magnetospheric plasma exchange.

A further clarification should be made about studies of the midlatitude trough. This clarification was first pointed out by Taylor and Walsh (1972) and concerns the importance of studying the trough signature in light ions as opposed to total ion (or electron) density. Taylor and Walsh were able to show that the light ion ionospheric trough, as seen in H^+ ions, was present at all

local times, as is the plasmopause, and therefore provides an improved way to study the trough-plasmopause association. This is particularly true in the dayside topside ionosphere where the high densities of the dominant photo-ionized O^+ ions tend to mask the changes in H^+ density expected at the ionospheric extension of the plasmopause. Although the work of Taylor and Walsh is important to studies of the trough it does not alleviate the problem of defining the precise trough position since even if one examines H^+ variations (as opposed to total ions or n_e), the range of latitudes covered by the decreasing density on the low latitude side of the light ion trough is large (see Figure 2). Nevertheless, if we adopt a trough position using the suggested definition of the low latitude point where there is an initial H^+ density decrease, the light ion trough position occurs at L-shells which are well inside the statistical plasmopause position. An example of this behavior can be seen, for example, in Taylor and Walsh, 1972, Figure 5, where the density decreases in light ions are found in the range of 30° to 50° dipole latitude.

Using the definitions discussed above, previous studies of the trough have reached the following conclusions: (1) On the nightside (local times of 2100 to 0600) the trough position and the plasmopause are close to the same field line and move to decreasing L-shells with increasing K_p [Rycroft and Thomas, 1970; Thomas and Andrews, 1968; Burnell and Rycroft, 1970]. (It should be noted that a definition of the trough was used which gives locations roughly two L-shells poleward of the initial low latitude, light ion density decrease.) (2) Using the light ions instead of the total density, the trough can be seen at all local times and is near the expected ionospheric projection of the plasmopause (Taylor and Walsh, 1972). (3) Using total electron density at high altitudes (>2500 km where H^+ is assumed to be the dominant ion) the trough is visible at all local times and appears to be circular at about $L=4$ displaying, in contradiction to

equatorial plasmasphere measurements, no bulge region (Brace and Theis, 1973).

From the foregoing, one finds that the trough and plasmopause appear to be co-located on the nightside, but, from (3) above, the trough appears not to exhibit the prominent bulge region seen in the outer plasmasphere at dusk.

Although real physical differences may exist between the ionospheric projection of the plasmopause and the trough, it is worthwhile to ask whether or not the lack of agreement is simply a matter of the ad hoc nature of the original definitions; i.e., if one uses a more physically meaningful definition of the trough, will there be an improvement in our understanding of the association between the trough and plasmopause? In the following work, our procedure will be to define the trough position as the point of initial decrease in light ion density on the low latitude side of the trough. Using this definition an examination is made of measurements of the midlatitude trough and plasmasphere in the light of current theories of thermal plasma flow.

Evidence of Disagreement Between the Midlatitude Trough and Plasmopause

Although we have already pointed out that the statistical studies of the trough - plasmopause connection are limited in their successes and challenged in their basic definitions, the evidence concerning the disagreement between trough and plasmopause position is only indirect. The first study showing this disagreement explicitly was made by Banks and Doupnik, 1973. (It was also alluded to in an earlier study by Brinton et al., 1971 in their discussion of a "transition region"). Banks and Doupnik examined Alouette II sounder data on the electron density profiles of the topside ionosphere (up to about 2500 km) near dawn. Using models of the topside ionosphere based on the momentum and continuity equation for O^+ and H^+ , they were able to interpret topside electron density profiles in terms of a large upward flow of H^+ ions. They found that this upward flow was present inside as well as outside the plasmopause and could

be found down to invariant latitudes as low as $50^\circ\Lambda$ ($L=2.5$). At this low latitude point there was evidence of a trough in the total electron density. But as Taylor and Walsh, (1972), pointed out, this is to be expected because of the masking effect of the dominant O^+ in the sunlit ionosphere. Part (b) of Figure 4 shows three topside density profiles measured at three different latitudes on the pass, $\Lambda=72^\circ$, 56° and 50° . As Banks and Doupnik point out, these profiles are consistent with there being a full flow of H^+ ions upward out of the topside ionosphere into the plasmasphere. This flow regime is generally expected in the plasma trough region outside the plasmopause (Brinton et al., 1971), but it is surprising to see it inside the plasmopause. Only in profile (3), which was measured at $\Lambda=50^\circ$ ($L=2.5$) (well inside the expected plasmopause position), does the upturn in the density profile near 2000 km occur. This upturn is evidence for a transition to a distribution where H^+ is in diffusive equilibrium.

It therefore appears from these data that the transition from a diffusive equilibrium distribution to a polar wind-like upward flow distribution can take place well inside the plasmopause. Apparently, the transition is not always at the plasmopause as has traditionally been thought and this should have an important influence on the trough position in the topside ionosphere. There must, then, be another boundary besides the plasmopause which influences the distribution of ionization in the topside ionosphere.

The Boundary Between the "Inner and Outer" Plasmasphere

The explanation for a transition from diffusive equilibrium to full flow ion distribution inside the plasmopause can be found by considering the filling state of the plasmasphere. In particular, it is necessary to ask if all of the flux tubes inside the plasmopause are full of plasma (and therefore in diffusive equilibrium) subject only to day-night ebb and flow or if some of the magnetic

field tubes in the outer portions of the plasmasphere are still in a state of filling. If the tubes of the outer plasmasphere have not come to diffusive equilibrium, then there can be large upward flows of ionization present on these flux tubes (an idea of the way filling proceeds is given by Banks et al., 1971).

Data on the degree of plasma filling in the outer plasmasphere has recently been presented by Park (1973). This information is derived from whistler data and gives the length of time required for the flux tubes inside the plasmasphere to reach a saturation level following a geomagnetic storm. Some of Park's recent data are shown in Figure 5. Here the measured total electron content of flux tubes ranging from L=2 out to L=6 are plotted as a function of time following an isolated magnetic storm which drove the plasmopause to L-shells as low as 2 or 2.5. The storm onset occurred on June 16, 1965. The curves show the subsequent tube content starting on June 18 and continuing through June 25. It is seen that as the tubes fill they eventually reach a saturation value of total electron content which increases with increasing L as a consequence of increasing flux tube volume.

An important aspect of these measurements is the number of days required for the flux tubes to reach a saturation content. Using correlated bottomside sounder data from several stations during this period Park has also found that the F_2 -peak of the ionosphere was able to recover to its average density in a period of about three days but it took up to eight days for the plasmasphere flux tubes near L=4 to reach saturation, and in this case the plasmopause itself is estimated to be outside of L=6. Therefore, we see data that following a magnetic storm there is a boundary established earthward (equatorward) of the post storm plasmopause inside of which the ionosphere and plasmasphere have reached a near diffusive equilibrium distribution and outside of which the flux

tubes are still filling with large upflows (Park has estimated the daytime upflow to be 3×10^8 ions/cm² sec at 1000 km with a nighttime downflow of 1.5×10^8 ions/cm² sec for this case). As illustrated in Figure 5, this boundary between the "inner and outer" plasmasphere expands gradually outward (and poleward) to higher L-shells. Note that the boundary is at L=2.5 on June 18 (2 days after the storm) at L=2.7 on the 19th, at L=2.9 on the 20th and so on. The precise position of the inner-outer plasmasphere transition can be quite variable but in general it should depend on: (1) the length of time since the previous magnetic storm and (2) the magnitude of the previous storm, i.e., the innermost penetration of the plasmopause.

Figure 6 shows a conceptual view of the thermal plasma regimes in the magnetosphere with the addition of the new boundary of the inner-outer plasmasphere. The innermost or lowest latitude region comprises the inner plasmasphere. Here, the flux tubes are "full" and have reached diffusive equilibrium. The outer boundary of this region is initially co-located at the storm time plasmopause position and moves outward as the plasmasphere fills and the plasmasphere and ionosphere come into diffusive equilibrium (or reach the "saturation level" as described by Park). Nevertheless, the inner-outer plasmasphere boundary does not always have to begin at the previous storm-time plasmopause. One can envisage a situation following a large magnetic storm where the inner-outer plasmasphere transition zone begins to move outward in response to filling during a very quiet period. Then, the onset of a very small magnetic storm could move the quiet time plasmopause inwards to lower L-shells but not completely into the inner-outer boundary which would continue to fill and move outwards.

The second zone shown in Figure 6 is the outer plasmasphere. Here the flux tubes are in a filling state with their plasma distribution in an inter-

mediate state between diffusive equilibrium and full flow. In this region there are large upward flows of H^+ each day even though they have significant densities of ions collected near the equatorial plane (See Park, 1973, Figure 3). The outer plasmasphere is bounded on the inside by the inner-outer plasmasphere transition, and on the outside by the plasmopause. If the global magnetic activity remains steady, the outer plasmasphere can gradually fill until the inner-outer plasmasphere boundary reaches the plasmopause position.

Outside the plasmopause the plasma trough is a region of full upward H^+ flow similar to the outer plasmasphere with the exception that in this region the flux-tubes are emptied approximately once each day in the afternoon-dusk sector by the effects of the magnetospheric convection electric field (see Review by Chappell, 1972). Although both the outer plasmasphere and plasma-trough regions are probably regions of full H^+ flow, the plasmopause position is still quite evident between them because of the loss of ionization each day in the plasmatrough and the steady accumulation of ionization in the outer plasmasphere.

Finally, the polar cap sector of open magnetic field line is also a full upward flow region (see Banks and Holzer, 1969). Here the ion flow is along open field lines and is a continual outflow with no accumulation in the equatorial regions as occurs in the other zones.

The Effects of the Inner-Outer Plasmasphere Boundary on the Topside Ionosphere

The upward plasma flows in the different regions shown in Figure 6 can have a significant effect upon ion and electron densities in the topside ionosphere. The expected effects are illustrated in Figure 7, taken from Banks and Doupnik, 1973. This figure shows the distribution of O^+ and H^+ as a function of altitude for a variety of flow conditions ranging from a downward flow of 2.3×10^8 ions/cm² sec at 3000 km to an upward flow of 1.35×10^8 ions/cm²

sec. The shaded area shows the range of the O^+ distribution of the different H^+ flows with the upper curve of the shaded area corresponding to the upward flow of H^+ of 1.35×10^8 ions/cm² sec. The details of the solution of the different flow distributions are given in Banks and Doupnik, 1973. Similar solutions have also been given by Mayr et al., 1970 and Brinton et al., 1971, to illustrate the changing topside ionosphere distribution at the plasmopause.

In Figure 7 the varying flows that are illustrated are a direct result of the external plasma pressure on the topside ionosphere. This varying pressure is a direct result of the degree to which the flux tubes have been filled and how the ionization has distributed itself along the field line during filling (see Mayr et al., 1970 and Banks et al., 1971, for a discussion of the filling). At 2500 km, for example, there can be over an order of magnitude change in the density as one goes from a zero upflow (arrow) to an upflow of 1.35×10^8 ions/cm² sec. Therefore, when a satellite at 2500 km passes from the inner plasmasphere to the outer plasmasphere, it passes from a diffusive equilibrium or low flow region to an intermediate filling region which still contains large upflows. As a consequence, at this boundary there should be a density drop of an order of magnitude or more.

This effect is schematically illustrated in Figure 8 where the expected 2500 km electron density is shown for increasing L-shells ranging from the inner plasmasphere into the plasmatrough and auroral zone. Within the inner plasmasphere the density remains relatively constant (excluding F_2 -region dynamical effects) until the inner-outer plasmasphere boundary is reached. Here the electron density drops sharply by over an order of magnitude as a result of the transition from H^+ diffusive equilibrium to a flow regime. Owing to uncertainty in the way plasmasphere refilling occurs, we have included two dashed curves as alternative ways in which the density fall off might

appear with increasing L. Until we can gain further information on the actual distribution of ionization along field lines in refilling regions we can only speculate on how the plasma pressure in the topside ionosphere should vary with L-value in the filling region of the outer plasmasphere. It may be possible, however, to use existing satellite data on the measured slope of the low latitude side of the trough to gain information about the pressure changes in the outer plasmasphere.

If the outer plasmasphere region is in full upward flow, there should be no trace of the plasmopause in the topside ionosphere. If the external pressure difference (parallel to the magnetic field lines) present at the plasmopause can be transmitted to the topside ionosphere, then there would be a change of flow with a corresponding change in topside density. Finally, the auroral zone and polar cap portion of the topside profile is strongly affected by variations in F_2 -layer density ionization caused by electron precipitation.

The effect of the inner-outer plasmasphere boundary in forming the low latitude edge of the topside ionospheric trough has been verified by at least one correlative study of the two regions. Part (a) of Figure 9 shows H^+ measurements from an outbound pass of OGO-5 through the plasmasphere in the afternoon sector at 0133 - 0251 UT on August 18, 1973. Part (b) of the figure shows an Alouette II pass over the same L-shells about two hours later in universal and local time. If one assumes approximate corotation of plasma at these lower L-shells, the two passes should be looking at very nearly the same flux tubes. We note that in the OGO-5 data there is a sudden drop in H^+ density at $L=2.6$ (giving evidence of a previous storm time plasmopause) and another drop at $L=6.5$ (the normal bulge region plasmopause). The drop at $L=2.6$ probably represents the boundary between the inner and outer plasmasphere which appears prominently in the Alouette II density data at $L=2.5$. This correlation verifies the close

connection between the midlatitude trough and the inner-outer plasmasphere boundary. The density drop of almost two orders of magnitude at $L=6.5$ in the OGO-5 data, however, is not obvious in the Alouette data. Clearly, in this case at least, the density variation which would be characterized as the midlatitude trough in the Alouette II data corresponds to the inner-outer plasmasphere boundary and not the equatorial plasmopause which falls at $L=6.5$.

The Relationship Between the Midlatitude Trough and the Plasmopause

It appears from the above discussion that the initial low latitude density decline associated with the midlatitude trough is the transition zone between the inner and outer plasmasphere. This boundary is only occasionally found at the plasmopause. The most favorable conditions for agreement between the plasmopause and the low latitude side of midlatitude trough probably occurs on the nightside when downflows from the plasmasphere into the ionosphere are present. In particular, at the onset of high magnetic activity when the plasmopause is driven to low L -values, the inner-outer boundary of the plasmasphere and the plasmopause are established simultaneously at about the same L -shell. A second possible set of circumstances leading to co-location of the plasmopause and trough could be after a long period of steady magnetic disturbance during which the inner-outer plasmasphere boundary has filled out to the corotation-convection boundary which creates the plasmopause. Such a situation would require that the plasmopause position remain steady during a complete filling time (about 5 to 8 days).

What is the significance of the dayside trough? In total ion/electron density it probably represents only the decrease in O^+ density with increasing latitude arising from a decreasing solar zenith angle on the low latitude side and the increase in density due to precipitation in the polar cusp on the high latitude side. In light ions the dayside trough probably is the signature of the inner-outer plasmasphere boundary which can be the same as the plasmopause

only for the special filling conditions discussed in the previous paragraph.

Does one expect a "bulge" in the midlatitude trough which is present in the plasmasphere? This does not appear to be the case for several reasons. First, the inner-outer plasmasphere boundary is generally found at relatively low L-shells ($L=2$ to 3) where corotation is the dominant influence on the drift of flux tubes. The convection electric field should have very little influence at these low L-shells and, consequently, the projection of this boundary would be nearly circular. Consequently, its signature in the ionosphere as the low latitude side of the trough should also be roughly circular. A second reason for a circular trough within the topside ionosphere may be associated with the fact that if the tubes of the inner plasmasphere did drift to higher L-shells in the dusk sector, their volumes would increase and the resulting lowering in pressure would induce an upflow of H^+ , thereby eliminating the trough signature.

Summary

In this paper we have introduced the effect on the topside ionosphere of the inner-outer plasmasphere boundary as defined by Park and have suggested that it is the dominant factor influencing the low latitude side of the mid-latitude ionospheric trough. It appears that the plasmopause and midlatitude trough are co-located only for special conditions and that previous statistical studies have failed to show this distinction because of somewhat arbitrary definitions of the trough position. The agreement between the point of initial density decrease on the low latitude side of the ionospheric trough has been substantiated in a limited number of cases through the use of OGO-5 and Alouette II correlative data.

ACKNOWLEDGEMENTS

The authors would like to thank Drs. L. Colin and K. L. Chan for furnishing the Alouette II electron density data used in this study. We also thank Dr. J. R. Doupnik for his work in processing the Alouette II data.

This work was supported, in part, by NSF Grant GA-33252.

BIBLIOGRAPHY

- Banks, P. M., Behavior of thermal plasma in the magnetosphere and topside ionosphere, Critical Problems of Magnetospheric Physics, Edited by E. R. Dyer, 1972.
- Banks, P. M. and J. R. Doupnik, Thermal proton flow in the plasmasphere: the morning sector, Planet. Space Sci., 21, 1973.
- Banks, P. M. and T. E. Holzer, High-latitude plasma transport: the polar wind, J. Geophys. Res., 1973.
- Banks, P. M., A. F. Nagy, and W. I. Axford, Dynamical behavior of thermal protons in the mid-latitude ionosphere and magnetosphere, Planet. Space Sci., 19, 1053, 1971.
- Brace, L. H. and R. F. Theis, The behavior of the plasmopause at mid-latitudes: ISIS-1 langmuir probe measurements, Goddard Preprint #X-621-73-220, 1973.
- Brinton, H. C., J. M. Grebowsky, and H. G. Mayr, Altitude variation of ion composition in the midlatitude trough region: evidence for upward plasma flow, J. Geophys. Res., 76, 3738, 1971.
- Carpenter, D. L., Whistler studies of the plasmopause in the magnetosphere, J. Geophys. Res., 71, 693, 1966.
- Chappell, C. R., Recent satellite measurements of the morphology and dynamics of the plasmasphere, Rev. of Geophys. and Space Physics, 10, No. 4, 951, 1972.
- Chappell, C. R., K. K. Harris, and G. W. Sharp, A study of the influence of magnetic activity on the location of the plasmopause as measured by Ogo 5, J. Geophys. Res., 75, 50, 1970.
- Mayr, H. G., J. M. Grebowsky, and H. A. Taylor, Jr., Study of the thermal plasma on closed field lines outside the plasmasphere, Planet. Space Sci., 18, 1123, 1970.
- Miller, N. J., The main electron trough during the rising solar cycle, J. Geophys. Res., 75, 7175, 1970.
- Muldrew, D. B., The latitudinal variation of the main trough with local time, Trans. Am. Geophys. Union, 51, No. 4, 1970.
- Muldrew, D. B., F-layer ionization troughs deduced from Alouette data, J. Geophys. Res., 70, 2635, 1965.
- Park, C. G., Some features of plasma distribution in the plasmasphere deduced from antarctic whistlers, Preprint submitted to J. Geophys. Res., 1973.
- Rycroft, M. J. and S. J. Burnell, Statistical analysis of movements of the ionospheric trough and the plasmopause, J. Geophys. Res., 75, 5600, 1970.
- Rycroft, M. J. and J. O. Thomas, The magnetospheric plasmopause and the electron density trough at the Alouette I orbit, Planet. Space Sci., 18, 65, 1970.

Sharp, G. W., Midlatitude trough in the night ionosphere, J. Geophys. Res., 71, 1345, 1966.

Taylor, H. A., H. C. Brinton, and A. R. Deshmukh, Observations of irregular structure in thermal ion distributions in the duskside magnetosphere, J. Geophys. Res., 75, 2481, 1970.

Taylor, H. A., Jr., and W. J. Walsh, The light-ion trough, the main trough, and the plasmopause, J. Geophys. Res., 77, 6716, 1972.

Thomas, J. O. and M. K. Andrews, Transpolar exospheric plasma, J. Geophys. Res., 73, 7407, 1968.

Figure Captions

Figure 1 - A sketch of the inner magnetosphere showing the plasmasphere and the ionosphere. The dashed line illustrates the path of a polar orbiting satellite in the topside ionosphere. A sketch of the expected topside density profile is shown in the top right-hand side of the figure. The dotted line illustrates an equatorial orbiting satellite pass through the equatorial plasmasphere with the expected density profile shown in the lower right-hand corner of the figure. The shaded region represents the plasmasphere.

Figure 2 - An example of ion density measurements in the topside ionosphere as measured by the mass spectrometer on the Ogo 4 polar orbiting satellite. The trough position is evident on each side of the equator at dipole latitudes of 40° to 70° .

Figure 3 - Three different definitions of the midlatitude ion trough position. Part (a) is taken from Rycroft and Thomas (1970) and uses the minimum point as the trough definition. Part (b) is from the work of Miller (1970) and uses the change in slope as the definition of the trough. Part (c) from Brace and Theis, 1973, uses the $1000 \text{ electron/cm}^3$ level as the trough position definition.

Figure 4 - Alouette II data taken from Banks and Doupnik (1973). Part (a) shows the density versus invariant latitude for several altitudes on a dawn (0821 local time) pass. Part (b) shows three electron density profiles in the topside ionosphere measured at three different invariant latitudes along the satellite pass, 72° , 56° and 50° .

Figure 5 - Whistler measurements from Park, 1973, on the refilling of the plasmasphere following the magnetic storm of June 16, 1965. This figure shows the total electron tube content as a function of L for successive days beginning June 18, 2 days following the storm. The tubes are seen to fill up to a saturation level shown by the heavy solid line.

Figure 6 - A sketch showing the different zones of thermal plasma density in the magnetosphere. In this sketch the inner plasmasphere has been added to the previously described regions of the outer plasmasphere, the plasmatrough, and the polar wind.

Figure 7 - A plot of the distribution of H^+ and O^+ ions in the topside ionosphere taken from Banks and Doupnik, 1973. The different distributions represent changing flux conditions at the 3000 km boundary level. The H^+ fluxes at 3000 km vary from 1.35×10^8 ions/cm² sec upward to 2.3×10^8 ions/cm² sec downward. The shaded region represents the variation in the O^+ profile for varying H^+ fluxes with the top curve of the shaded region representing an upward H^+ flux of 1.35×10^8 ions/cm² sec. The diffusive equilibrium or zero flux H^+ profile is shown by the arrow.

Figure 8 - A sketch of the expected ion density variations in the topside ionosphere. The density drops significantly at the boundary between the inner and outer plasmasphere. The exact nature of the drop with increasing L is unknown because of the unknown filling distribution of ionization along the magnetic field in the outer plasmasphere and plasmatrough. The high latitude increase in ionization is due to auroral precipitation.

Figure 9 - OGO-5 and Alouette II correlative data taken on August 18, 1973 showing the inner-outer plasmasphere boundary signature in both the plasmasphere and topside ionosphere. In this refilling situation this boundary is seen to occur at about L=2.6 well inside the plasmopause boundary at L=6.5.

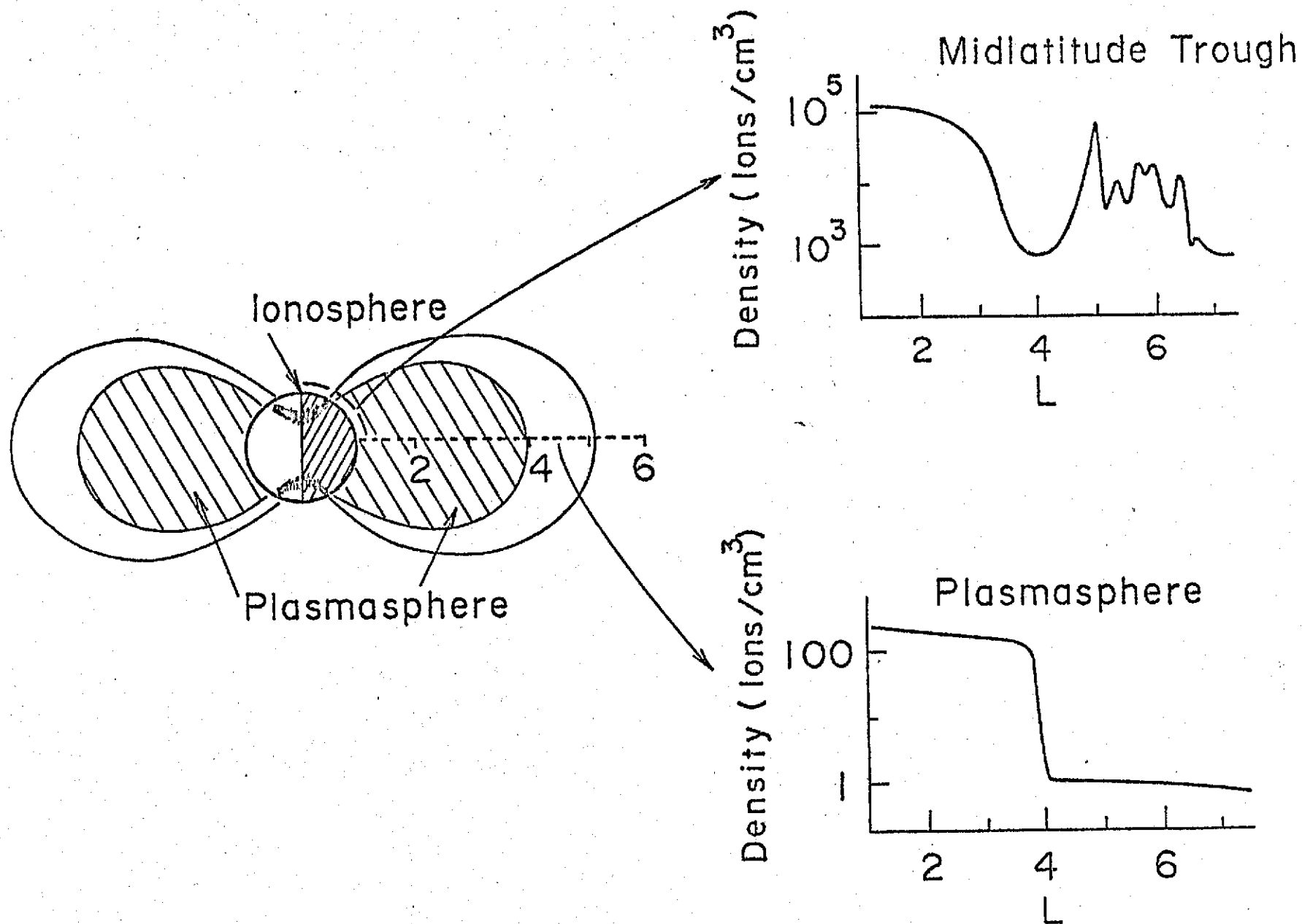


Figure 1

OGO-4 SEPT. 13, 1967 1457-1547 U.T.

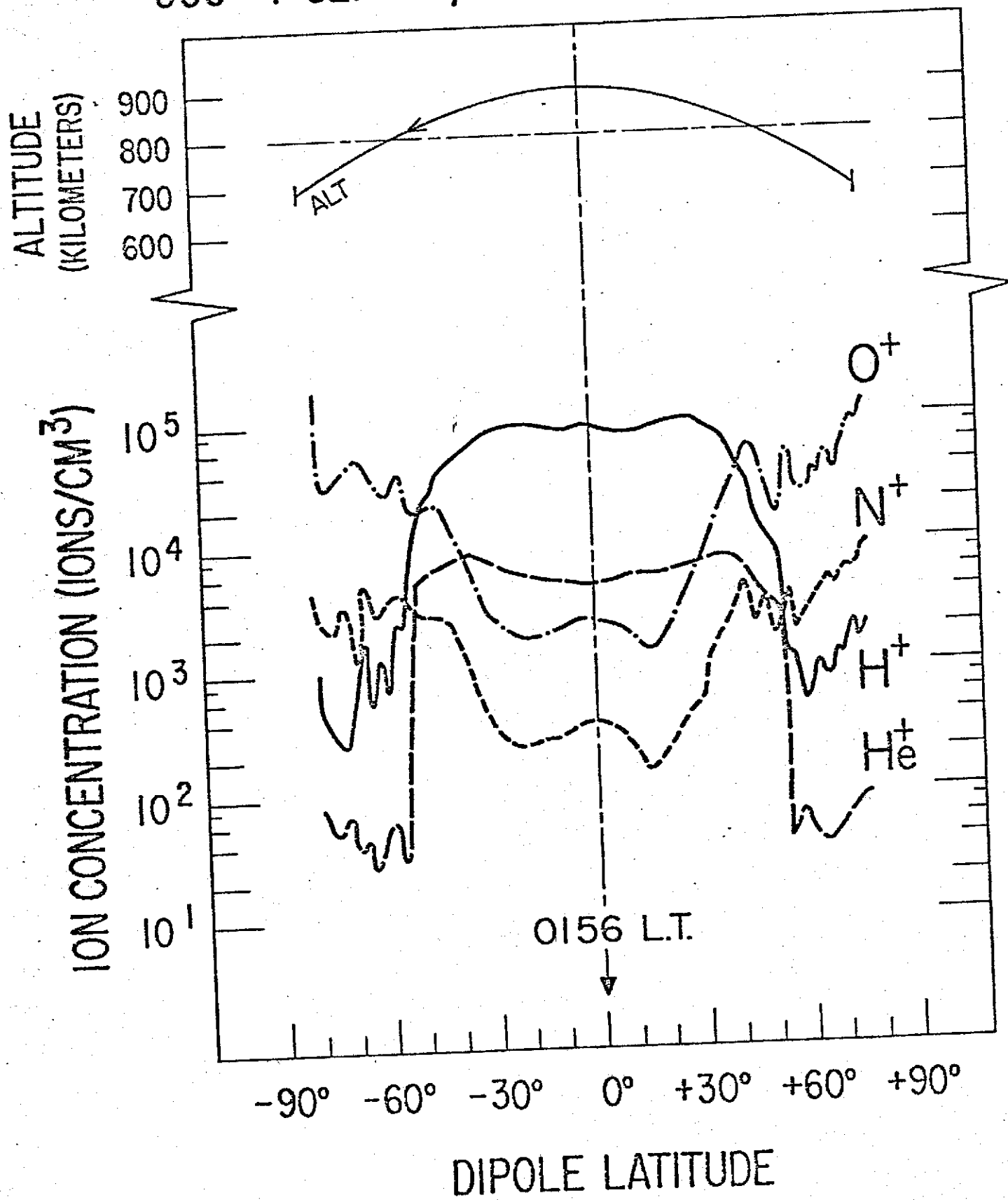
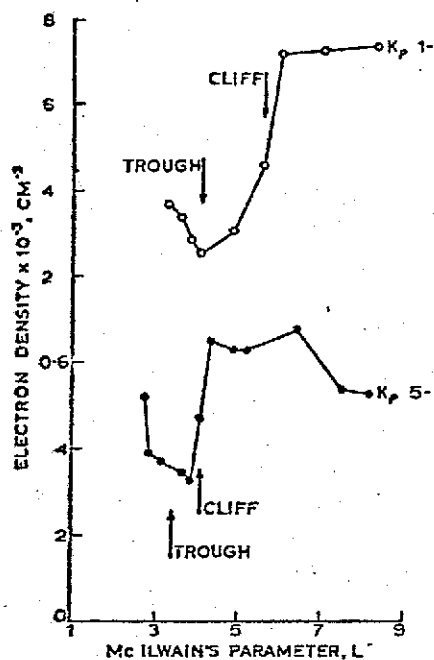
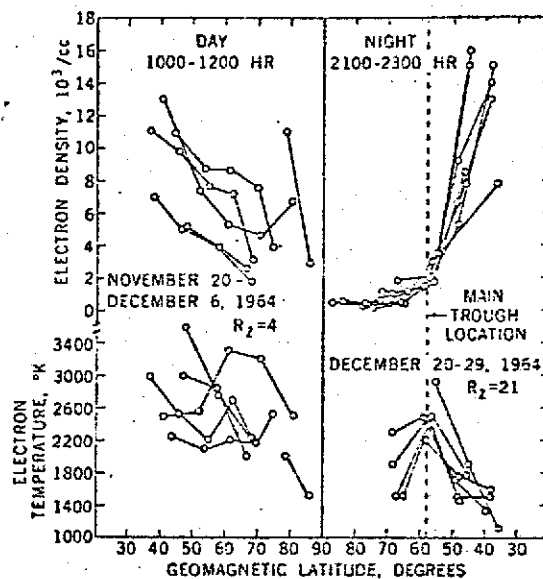


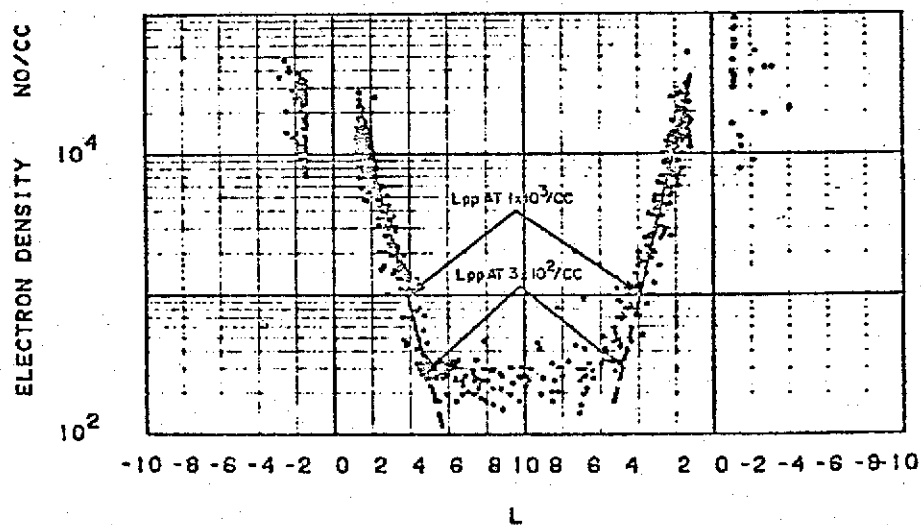
Figure 2



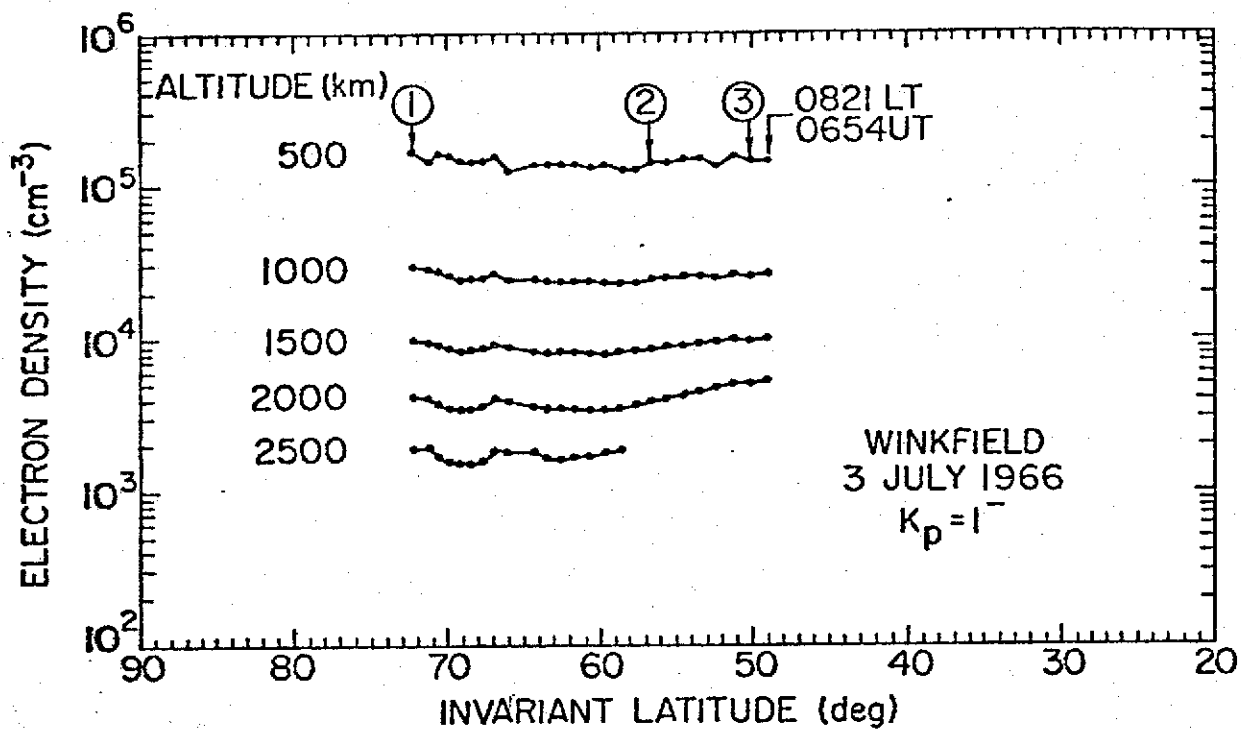
(a) Minimum



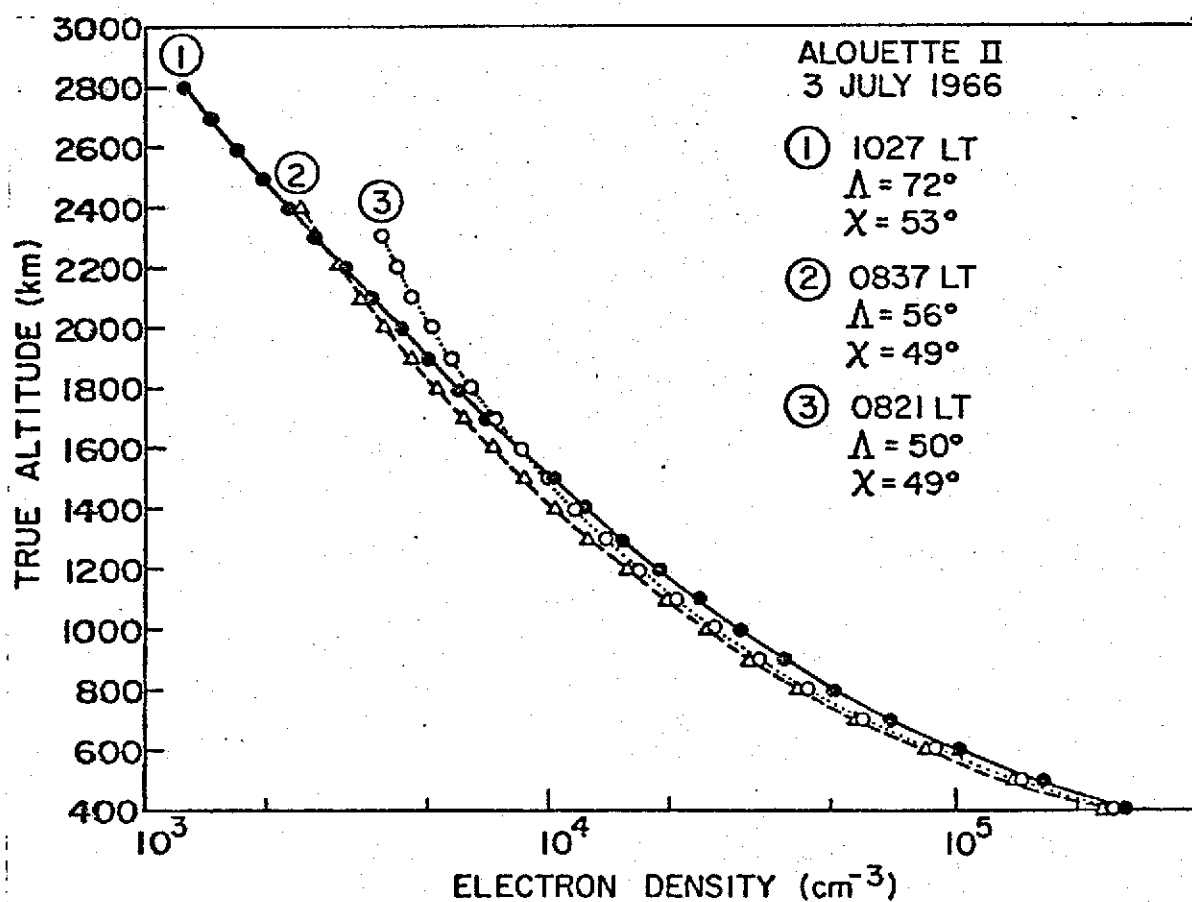
(b) Slope Change



(c) 1000 elec / cm³ Level



(a)



(b)

Figure 4

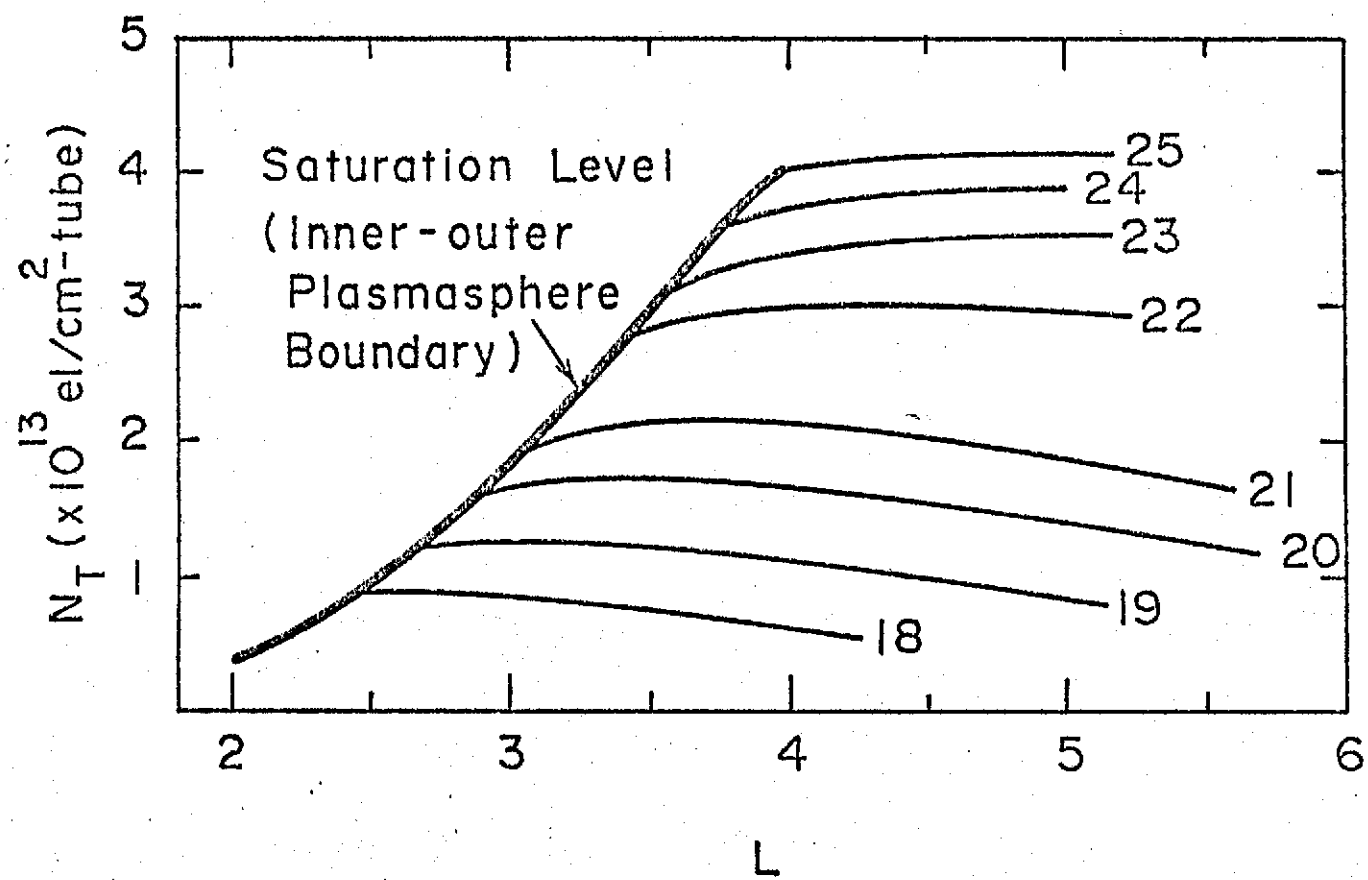


Figure 5

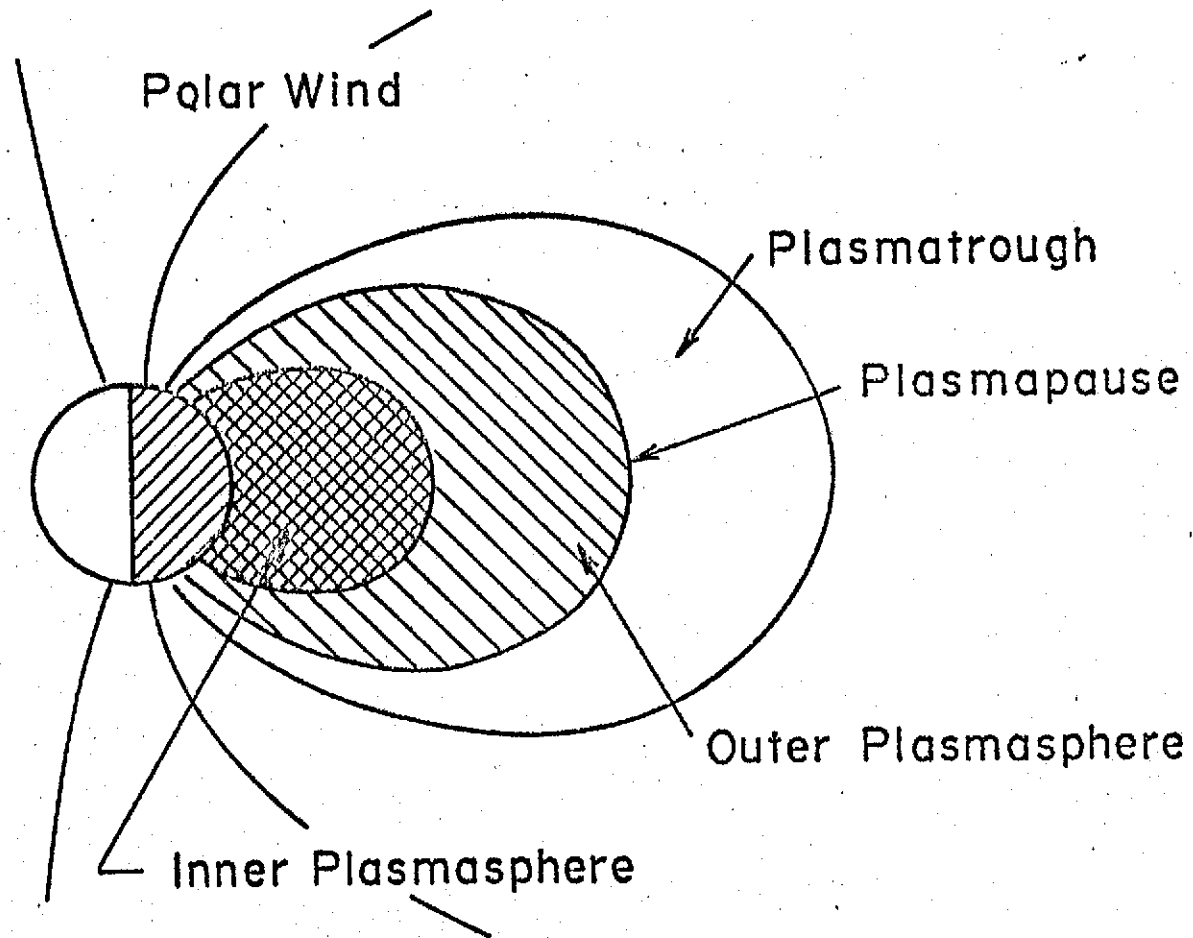


Figure 6

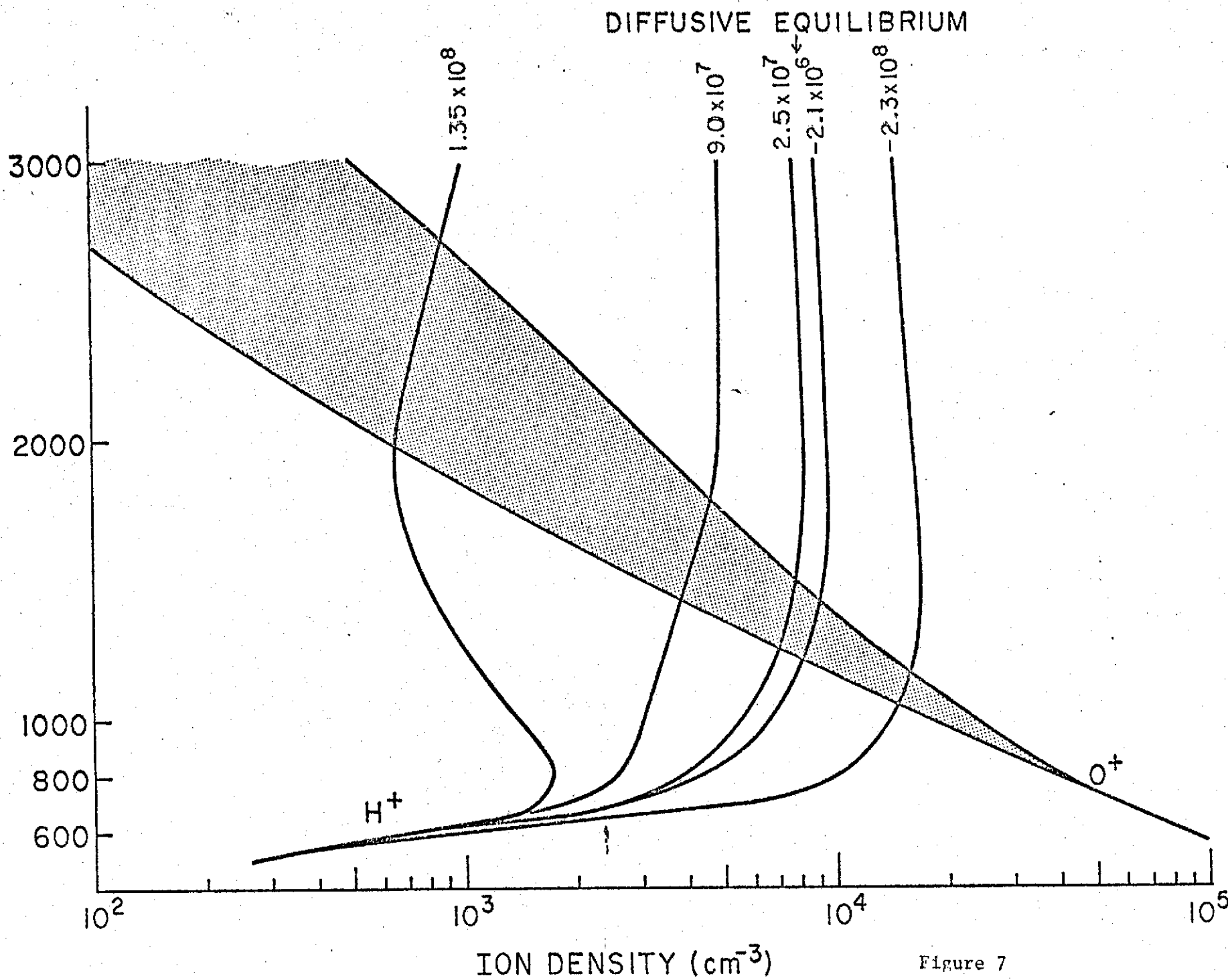


Figure 7

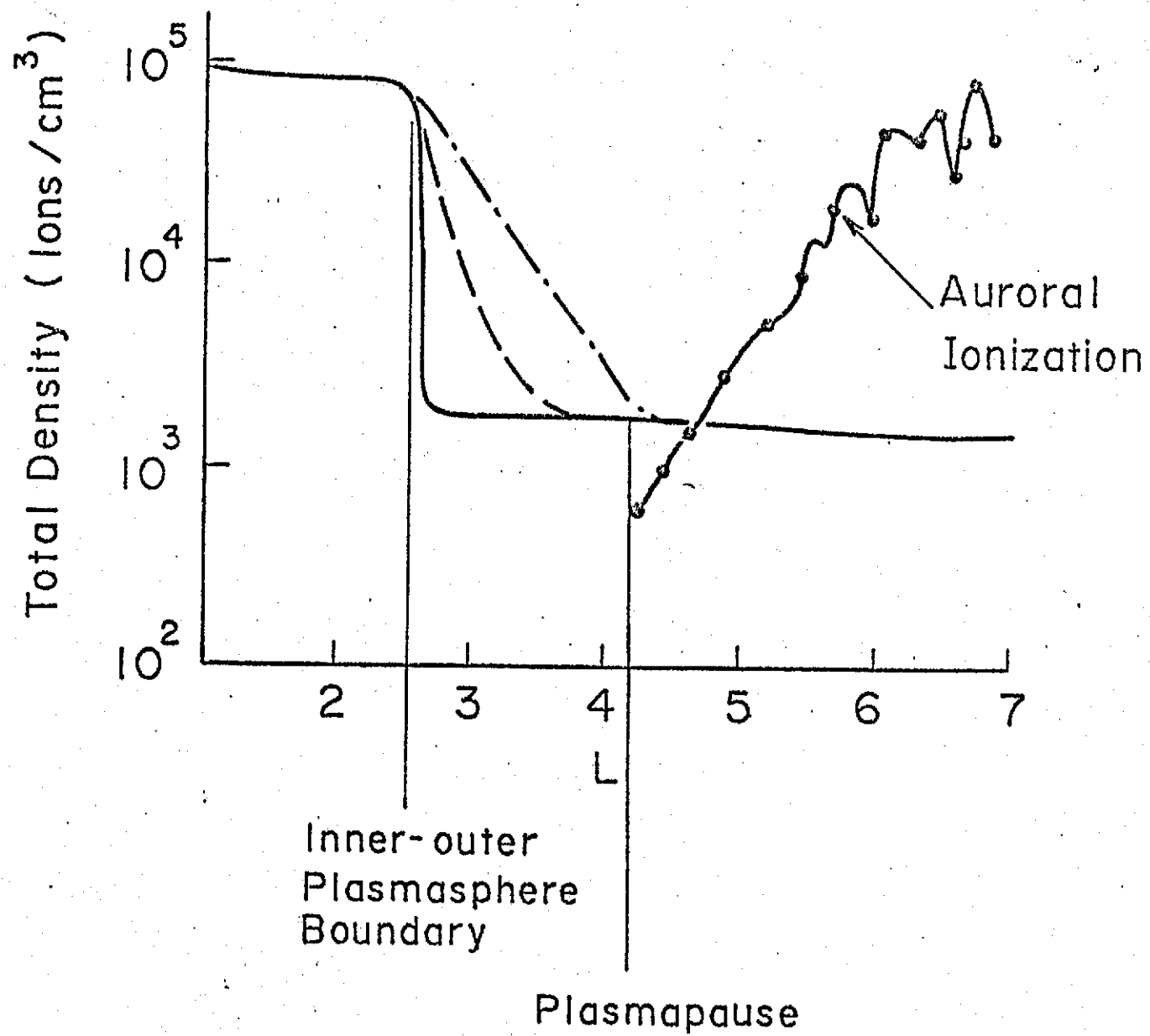
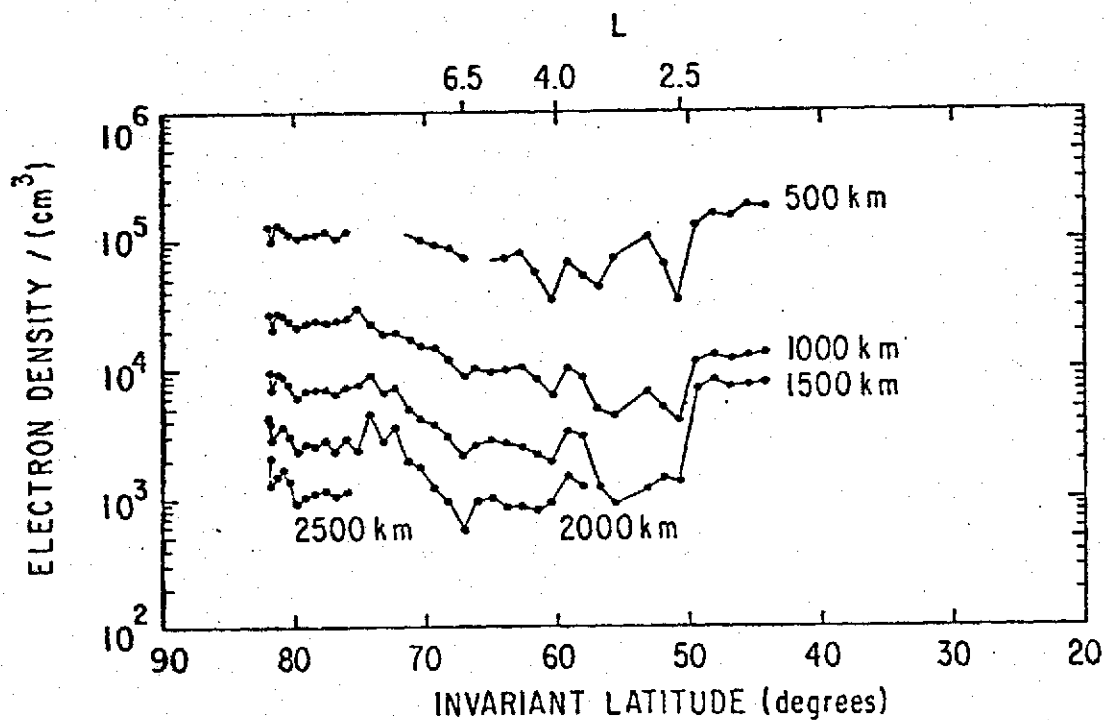
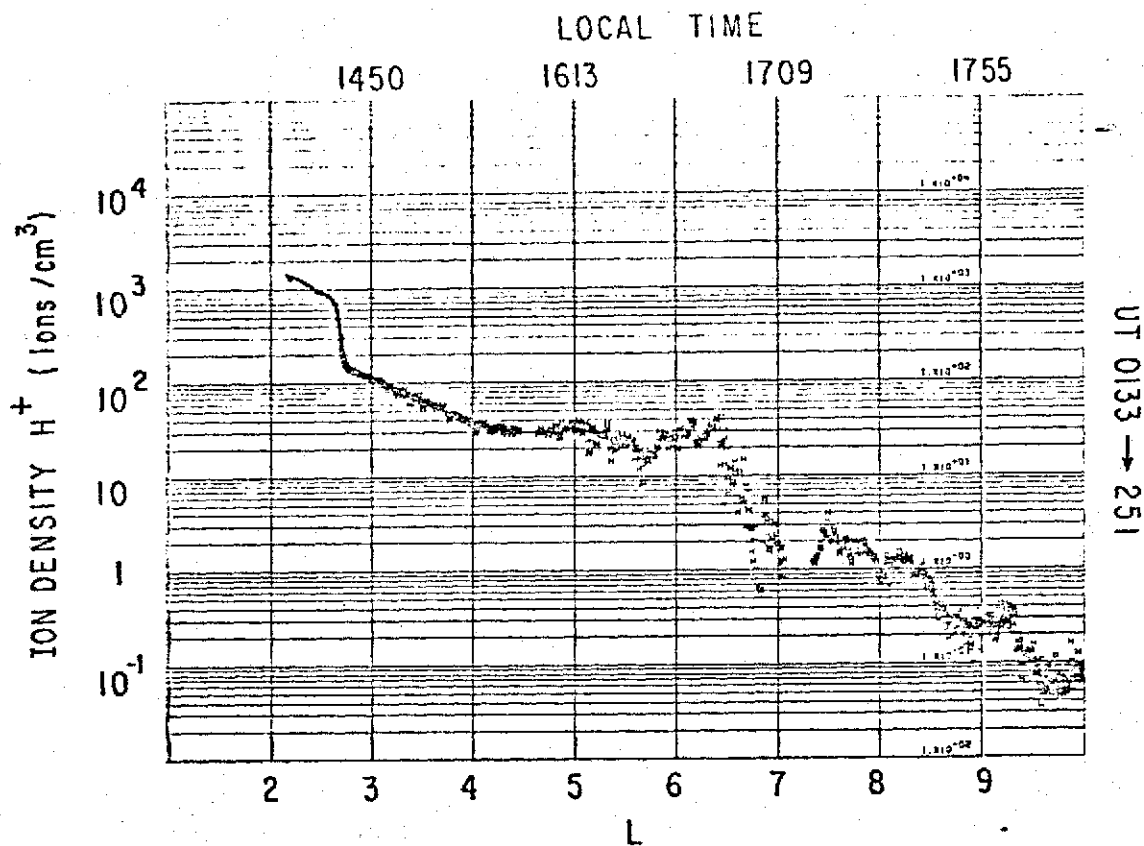


Figure 8



DATE (DMY) 18-8-68 START TIMES UT = 0423 LT = 2015

STATION 50 KP = 4 NORMALIZED AT Z

Figure 9